Institute of Physics Publishing Journal of Physics: Conference Series **53** (2006) 44–82
doi:10.1088/1742-6596/53/1/003 Corfu Summer Institute on Elementary Particle Physics

Neutrino mass and New physics

A. Yu. Smirnov
International Centre for Theoretical Physics,
Strada Costiera 11, Trieste, Italy
Institute for Nuclear Research, RAS, Moscow, Russia

E-mail: smirnov@ictp.trieste.it

Abstract.
Reconstruction of the neutrino mass and flavor spectrum is described. Essentially two processes are relevant for interpretation of the neutrino results which were used in determination of neutrino parameters: oscillations (averaged and non-averaged) in vacuum and matter and the adiabatic flavor conversion in matter (the MSW-effect). Detailed physics picture of these processes is elaborated and their realizations in solar and atmospheric neutrinos as well as in K2K, KamLAND and MINOS experiments are described. Important bounds have been obtained from neutrinoless double beta decay and cosmology. Implications of the obtained results to fundamental physics are discussed. Among various mechanisms for small neutrino masses we consider the seesaw (which has the highest priority) and overlap suppression in extra dimensions. The observed pattern on neutrino mixing may testify for existence of new symmetries of nature. One of the key issues on the way to underlying physics is comparison of the quarks and lepton masses and mixing. In this connections concepts of quark-lepton symmetry and unification, quark-lepton universality and quark-lepton complementarity are described.

1. Introduction

The central issue of these lectures is the neutrino mass and lepton mixing, non-standard neutrino interactions.

Neutrino mass is considered as the first manifestation of physics beyond the standard model, as a window to new physics. What is this New physics? What do we see in the window? How far beyond?

The statement requires some clarification. The quark and lepton mass hierarchies as well as the structure of CKM mixing have no explanation in the Standard Model either. And in this sense they are also manifestations of physics beyond SM.

Quark mass and mixing as well as neutrino mass and mixing are new physics. Some part of this new physics may be in common. At the same time, neutrinos may require something more.

The bottom line is that new physics behind the neutrino masses and mixing has not been identified yet. It is difficult to say with confidence what is correct context or domain of new physics involved. There are plenty of models, scenarios and approaches and only few simplest possibilities have been excluded so far. Typically models accommodate but not really explain the results. And we can argue only what is the most plausible possibility.

Two zeros. The main salient feature of neutrinos is the neutrality:

$$Q_\gamma = Q_c = 0. \qquad (1)$$

So it would be natural to explain all unusual properties of neutrinos using this feature. The neutrality opens the following possibilities:

- neutrinos can be Majorana particles, and therefore have the Majorana mass terms;
- they can mix with singlets of the SM symmetry group;
- the right-handed components (RH), if exist, are singlets of $SU(3) \times SU(2) \times U(1)$. So, their masses are unprotected by the symmetry and therefore can be large: $M_R \gg v_{EW}$, where v_{EW} is the electroweak scale.

In turn, properties of the RH components allow them to propagate in extra dimensions, or be located on the "hidden" (not ours) brane in contrast to other fermions, *etc.*.

Introduction of the RH neutrino has a number of attractive features [1], in particular, it allows one to extend the electroweak symmetry to the gauged $SU(2)_L \times SU(2)_R \times U(1)_{B-L}$.

Is this enough to explain the properties of the mass spectrum and mixings?

Window to hidden world Neutrinos are the only known fermions which which can mix with particles from the hidden sector (related *e.g.* to SUSY or strings or mirror world). Properties of the neutrino mass and mixing can be associated to this mixing.

In the first part of the course I will explain how neutrino parameters (masses and mixing) have been determined. I will argue why we are confident that the interpretation in terms of vacuum masses and mixing is correct.

In the second part I will review analysis of these results and their possible implications.

2. Notions and notations

2.1. Flavors, masses and mixing

The *flavor* neutrino states: $\nu_f \equiv (\nu_e, \nu_\mu, \nu_\tau)$ are defined as the states which correspond to certain charge leptons: e, μ and τ. The correspondence is established by weak interactions: ν_l and l ($l = e, \mu, \tau$) form the charged currents. It is not excluded that additional neutrino states, the sterile neutrinos, ν_s, exist. The neutrino *mass states*, ν_1, ν_2, and ν_3, with masses m_1, m_2, m_3 are the eigenstates of mass matrix as well as the eigenstates of the total Hamiltonian in vacuum.

The *vacuum mixing* means that the flavor states do not coincide with the mass eigenstates. The flavor states are combinations of the mass eigenstates:

$$\nu_l = U_{li}\nu_i, \quad l = e, \mu, \tau, \quad i = 1, 2, 3, \tag{2}$$

where the mixing parameters U_{li} form the PMNS mixing matrix U_{PMNS} [2, 3].

The mixing matrix can be conveniently parameterized as

$$U_{PMNS} = V_{23}(\theta_{23})V_{13}(\theta_{13})I_\delta V_{12}(\theta_{12}), \tag{3}$$

where V_{ij} is the rotation matrix in the ij-plane, θ_{ij} is the corresponding angle and $I_\delta \equiv diag(1, 1, e^{i\delta})$ is the matrix of CP violating phase.

2.2. Two aspects of mixing.

Many conceptual points can be clarified using just 2ν mixing. Also at the present level of accuracy of measurements the 2ν dynamics is enough to describe the data. For two neutrino mixing, *e.g.* $\nu_e - \nu_a$, we can write:

$$\nu_e = \cos\theta\ \nu_1 + \sin\theta\ \nu_2, \quad \nu_a = \cos\theta\ \nu_2 - \sin\theta\ \nu_1, \tag{4}$$

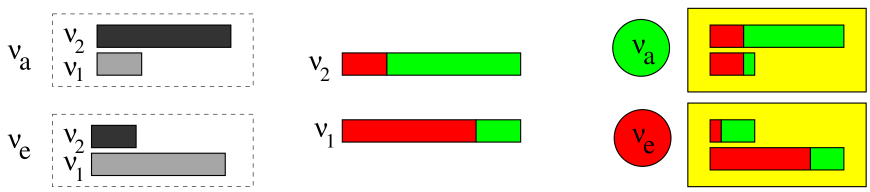

a). b). c).

Figure 1. a). Representation of the flavor neutrino states as the combination of the mass eigenstates. The length of the box gives the admixture of (or probability to find) corresponding mass state in a given flavor state. (The sum of the lengths of the boxes is normalized to 1. b). Flavor composition of the mass eigenstates. The electron flavor is shown by red (dark) and the non-electron flavor by green (grey). The sizes of the red and green parts give the probability to find the electron and non-electron neutrino in a given mass state. c). Portraits of the electron and non-electron neutrinos: shown are representations of the electron and non-electron neutrino states as combinations of the eigenstates for which, in turn, we show the flavor composition.

where ν_a is the non-electron neutrino state, and θ is the vacuum mixing angle.

There are two important physical aspects of mixing. According to (4) the flavor neutrino states are combinations of the mass eigenstates. One can think in terms of wave packets. Then propagation of ν_e (ν_a) is described by a system of two wave packets which correspond to ν_1 and ν_2.

In fig. 1a). we show representation of ν_e and ν_a as the combination of mass states. The lengths of the boxes, $\cos^2\theta$ and $\sin^2\theta$, give the *admixtures* of ν_1 and ν_2 in ν_e and ν_a.

The key point is that the flavor states are *coherent* mixtures (combinations) of the mass eigenstates. The *relative phase* or phase difference of ν_1 and ν_2 in ν_e as well as ν_a is fixed: according to (4) it is zero in ν_e and π in ν_a. Consequently, there are certain *interference* effects between ν_1 and ν_2 which depend on the relative phase.

Second aspect: the relations (4) can be inverted:

$$\nu_1 = \cos\theta\ \nu_e - \sin\theta\ \nu_a, \quad \nu_2 = \cos\theta\ \nu_a + \sin\theta\ \nu_e. \tag{5}$$

In this form they determine the *flavor composition* of the mass states (eigenstates of the Hamiltonian), or shortly, the flavors of eigenstates. According to (5) the probability to find the electron flavor in ν_1 is given by $\cos^2\theta$, whereas the probability that ν_1 appears as ν_a equals $\sin^2\theta$. This flavor decomposition is shown in fig. 1b). by colors (different shadowing).

Inserting the flavor decomposition of mass states in the representation of the flavors states, we get the "portraits" of the electron and non-electron neutrinos fig. 1c). According to this figure, ν_e is a system of two mass eigenstates which in turn have a composite flavor. On the first sight the portrait has a paradoxical feature: there is the non-electron (muon and tau) flavor in the electron neutrino! The paradox has the following resolution: in the ν_e- state the ν_a-components of ν_1 and ν_2 are equal and have opposite phases. Therefore they cancel each other and the electron neutrino has pure electron flavor as it should be. The key point is interference: the interference of the non-electron parts is destructive in ν_e. The electron neutrino has a "latent" non-electron component which can not be seen due to particular phase arrangement. However during propagation the phase difference changes and the cancellation disappears. This leads to an appearance of the non-electron component in propagating neutrino state which was originally produced as the electron neutrino. This is the mechanism of neutrino oscillations. Similar consideration holds for the ν_a state.

3. Two effects

3.1. To determination of oscillation parameters

In the Table 1 we show parameters to be determined, sources of information for their determination and physical effects involved. In the first approximation (when 1-3 mixing is neglected) the three neutrino problem splits into two neutrino problems and parameters of the 1-2 and 2-3 sectors can be determined independently.

Essentially two effects are relevant for interpretation of the present data in the lowest approximation:

- vacuum oscillations (both averaged and non-averaged)[2, 3, 4];
- adiabatic conversion in medium [5, 6].

Furthermore the 2ν mixing effects are enough. Notice that in the next order, when sub-leading effects are included, the problem becomes much more difficult and degeneracy of parameters appear. We will comment on this later.

3.2. Neutrino oscillation in vacuum

In vacuum the neutrino mass states are the eigenstates of the Hamiltonian. Therefore dynamics of propagation has the following features:

- Admixtures of the eigenstates (mass states) in a given neutrino state do not change. In other words, there is no $\nu_1 \leftrightarrow \nu_2$ transitions. ν_1 and ν_2 propagate independently. The admixtures are determined by mixing in a production point (by θ, if pure flavor state is produced).
- Flavors of the eigenstates do not change. They are also determined by θ. Therefore the picture of neutrino state (fig. 1 c) does not change during propagation.
- Relative phase (phase difference) of the eigenstates monotonously increases.

The phase is the only operating degree of freedom and we will consider it here in details.

Phase difference. Due to difference of masses, the states ν_1 and ν_2 have different phase velocities $v_{phase} = E_i/p_i \approx 1 + m_i^2/2E^2$ (for ultrarelativistic neutrinos), so that

$$\Delta v_{phase} \approx \frac{\Delta m^2}{2E}, \quad \Delta m^2 \equiv m_2^2 - m_1^2. \tag{6}$$

The phase difference changes as

$$\Delta\phi = \Delta v_{phase} t. \tag{7}$$

Table 1. Parameters and effects.

Parameters	Source of information	Physics effect
Δm_{12}^2, θ_{12}	Solar neutrinos	Adiabatic conversion
		Averaged vacuum oscillations
	KamLAND	Non-averaged vacuum oscillations
Δm_{23}^2, θ_{23}	Atmospheric neutrinos	Vacuum oscillations
	K2K	Vacuum oscillations
θ_{13}	CHOOZ	Vacuum oscillations
	Atmospheric neutrinos	oscillations in matter

Explicitly, in the plane wave approximation we have the phases of two mass states as $\phi_i = E_i t - p_i x$. Apparently, to find the phase difference which determines the interference effect one should take the phases of mass states in the same space-time point:

$$\phi \equiv \phi_1 - \phi_2 = \Delta E t - \Delta p x. \tag{8}$$

Since $p = \sqrt{E^2 - m^2}$, we have

$$\Delta p = \frac{dp}{dE}\Delta E + \frac{dp}{dm^2}\Delta m^2 = \frac{1}{v_g}\Delta E - \frac{\Delta m^2}{2p}, \tag{9}$$

where $v_g = dE/dp$ is the group velocity. Plugging (9) into (8) we obtain

$$\phi = \Delta E \left(t - \frac{x}{v_g} \right) + \frac{\Delta m^2}{2p} x. \tag{10}$$

Depending on physical conditions either $\Delta E \approx 0$ or/and $(t - x/v_g)$ is small which imposes the bound on size of the wave packet. As a consequence, the first term is small and we reproduce the result (7).

Increase of the phase leads to oscillations. Indeed, the change of phase modifies the interference: in particular, cancellation of the non-electron parts in the state produced as ν_e disappears and the non-electron component becomes observable. The process is periodic: when $\Delta\phi = \pi$, the interference of non-electron parts is constructive and at this point the probability to find ν_a is maximal. Later, when $\Delta\phi = 2\pi$, the system returns to its original state: $\nu(t) = \nu_e$. The oscillation length is the distance at which this return occurs:

$$l_\nu = \frac{2\pi}{v_{phase}} = \frac{4\pi E}{\Delta m^2}. \tag{11}$$

The depth of oscillations A_P is determined by the mixing angle. It is given by maximal probability to observe the "wrong" flavor ν_a. From the fig. 1c. one finds immediately (summing up the parts with the non-electron flavor in the amplitude)

$$A_P = (2 \sin\theta \cos\theta)^2 = \sin^2 2\theta. \tag{12}$$

Putting things together we obtain expression for the transition probability

$$P = A_P \left(1 - \cos \frac{2\pi L}{l_\nu} \right) = \sin^2 2\theta \sin^2 \frac{\Delta m^2 L}{4E}. \tag{13}$$

The oscillations are the effect of the phase increase which changes the interference pattern. The depth of oscillations is the measure of mixing.

3.3. Evolution equation

In vacuum the mass states are the eigenstates of Hamiltonian. So, their propagation is described by independent equations

$$i d\nu_i/dt = E_i \nu_i \approx (p_i + m_i^2/2p_i)\nu_i,$$

where we have taken ultrarelativistic limit and omitted the spin variables which are irrelevant for these oscillations. In the matrix form for three neutrinos $\nu \equiv (\nu_1, \nu_2, \nu_3)^T$, we can write

$$i\frac{d\nu}{dt} \approx \left(pI + \frac{|M_{diag}|^2}{2E} \right) \nu, \tag{14}$$

where $M^2_{diag} = diag(m_1^2, m_2^2, m_3^2)$. Using the relation $\nu = U^\dagger_{PMNS}\nu_f$ (2), we can write the equation for the flavor states:

$$i\frac{d\nu_f}{dt} \approx \frac{|M|^2}{2E}\nu_f, \tag{15}$$

where $M^2 = U_{PMNS}|M_{diag}|^2 U^\dagger_{PMNS}$ is the mass matrix squared in the flavor basis. In (15) we have omitted the term proportional to the unit matrix which does not produce any phase difference and can be absorbed in the renormalization of the neutrino wave functions. So, the Hamiltonian of the neutrino system in vacuum is

$$H_0 = \frac{|M|^2}{2E}. \tag{16}$$

In the 2ν mixing case we have explicitly:

$$H_0 = \frac{\Delta m^2}{4E}\begin{pmatrix} -\cos 2\theta & \sin 2\theta \\ \sin 2\theta & \cos 2\theta \end{pmatrix}. \tag{17}$$

Solution of the equation (15) with this Hamiltonian leads to the standard oscillation formula (13).

3.4. Matter effect

Refraction. In matter, neutrino propagation is affected by interactions. At low energies the *elastic forward scattering* is relevant only (inelastic interactions can be neglected) [5]. It can be described by the potentials V_e, V_a. In usual medium difference of the potentials for ν_e and ν_a is due to the charged current scattering of ν_e on electrons ($\nu_e e \to \nu_e e$) [5]:

$$V = V_e - V_a = \sqrt{2}G_F n_e\ , \tag{18}$$

where G_F is the Fermi coupling constant and n_e is the number density of electrons. The result follows straightforwardly from calculation of the matrix element $V = \langle\Psi|H_{CC}|\Psi\rangle$, where Ψ is the state of medium and neutrino. Equivalently, one can describe the effect of medium in terms of the refraction index: $n_{ref} - 1 = V/p$.

The difference of the potentials leads to an appearance of additional phase difference in the neutrino system: $\phi_{matter} \equiv (V_e - V_a)t$. The difference of potentials (or refraction indexes) determines the *refraction length*:

$$l_0 \equiv \frac{2\pi}{V_e - V_a} = \frac{\sqrt{2}\pi}{G_F n_e}. \tag{19}$$

l_0 is the distance over which an additional "matter" phase equals 2π.

In the presence of matter the Hamiltonian of system changes:

$$H_0 \to H = H_0 + V, \tag{20}$$

where H_0 is the Hamiltonian in vacuum. Using (16) we obtain (for 2ν mixing)

$$H = \frac{|M|^2}{2E} + V, \qquad V = diag(V, 0). \tag{21}$$

The evolution equation for the flavor states in matter then becomes

$$i\frac{d\nu_f}{dt} = \left[\frac{\Delta m^2}{4E}\begin{pmatrix} -\cos 2\theta & \sin 2\theta \\ \sin 2\theta & \cos 2\theta \end{pmatrix} + V\right]\nu_f. \tag{22}$$

The eigenstates and the eigenvalues change:

$$\nu_1, \;\; \nu_2 \;\; \rightarrow \;\; \nu_{1m}, \;\; \nu_{2m}, \tag{23}$$

$$\frac{m_1^2}{2E}, \;\; \frac{m_2^2}{2E} \;\; \rightarrow \;\; H_{1m}, \;\; H_{2m}. \tag{24}$$

The mixing in matter is determined with respect to the eigenstates of the Hamiltonian in matter ν_{1m} and ν_{2m}. Similarly to (4) the mixing angle in matter, θ_m, gives the relation between the eigenstates in matter and the flavor states:

$$\nu_e = \cos\theta_m \nu_{1m} + \sin\theta_m \nu_{2m}, \quad \nu_a = \cos\theta_m \nu_{2m} - \sin\theta_m \nu_{1m}. \tag{25}$$

The angle θ_m in matter is obtained by diagonalization of the Hamiltonian in matter (21)

$$\sin^2 2\theta_m = \frac{\sin^2 2\theta}{(\cos 2\theta - 2VE/\Delta m^2)^2 + \sin^2 2\theta}. \tag{26}$$

In matter both the eigenstates and the eigenvalues, and consequently, the mixing angle depend on matter density and neutrino energy. It is this dependence activates new degrees of freedom of the system and leads to qualitatively new effects.

Resonance. Level crossing. According to (26), the dependence of the effective mixing parameter in matter, $\sin^2 2\theta_m$, on density, neutrino energy as well as the ratio of the oscillation and refraction lengths:

$$x \equiv \frac{l_\nu}{l_0} = \frac{2EV}{\Delta m^2} \propto E n_e \tag{27}$$

has a resonance character. At

$$l_\nu = l_0 \cos 2\theta \qquad \text{(resonance condition)} \tag{28}$$

the mixing becomes maximal: $\sin^2 2\theta_m = 1$. For small vacuum mixing the condition (28) reads:

$$Oscillation \;\; length \;\; \approx \;\; Refraction \;\; length. \tag{29}$$

That is, the eigen-frequency which characterizes a system of mixed neutrinos, $1/l_\nu$, coincides with the eigen-frequency of medium, $1/l_0$.

For large vacuum mixing (for solar LMA: $\cos 2\theta = 0.4 - 0.5$) there is a significant deviation from the equality (29). Large vacuum mixing corresponds to the case of strongly coupled system for which, as usual, the shift of frequencies occurs.

The resonance condition (28) determines the resonance density:

$$n_e^R = \frac{\Delta m^2}{2E} \frac{\cos 2\theta}{\sqrt{2} G_F} \; . \tag{30}$$

The width of resonance on the half of the height (in the density scale) is given by

$$2\Delta n_e^R = 2 n_e^R \tan 2\theta. \tag{31}$$

Similarly, one can introduce the resonance energy and the width of resonance in the energy scale.

In medium with varying density, the layer where the density changes in the interval

$$n_e^R \pm \Delta n_e^R \tag{32}$$

is called the resonance layer.

In resonance, the level splitting (difference of the eigenstates $H_{2m} - H_{1m}$) is minimal [7, 8] and therefore the oscillation length being inversely proportional the level spitting, is maximal.

3.5. Oscillations in matter. Resonance enhancement of oscillations
In medium with constant density the mixing is constant: $\theta_m(E,n) = const$. Therefore

- the flavors of the eigenstates do not change;
- the admixtures of the eigenstates do not change; there is no $\nu_{1m} \leftrightarrow \nu_{2m}$ transitions, ν_{1m} and ν_{2m} are the eigenstates of propagation;
- monotonous increase of the phase difference between the eigenstates occurs: $\Delta\phi_m = (H_{2m} - H_{1m})t$.

This is similar to what happens in vacuum. The only operative degree of freedom is again the phase. Therefore, as in vacuum, the evolution of neutrino has a character of oscillations. However, parameters of oscillations (length, depth) differ from the parameters in vacuum. They are determined by the mixing in matter and by the effective energy splitting in matter:

$$\sin^2 2\theta \to \sin^2 2\theta_m, \qquad l_\nu \to l_m = \frac{2\pi}{H_{2m} - H_{1m}}. \tag{33}$$

For a given density of matter the parameters of oscillations depend on the neutrino energy which leads to a characteristic modification of the energy spectra. Suppose a source produces the ν_e- flux $F_0(E)$. The flux crosses a layer of length, L, with a constant density n_e and then detector measures the electron component of the flux at the exit from the layer, $F(E)$. In fig. 2

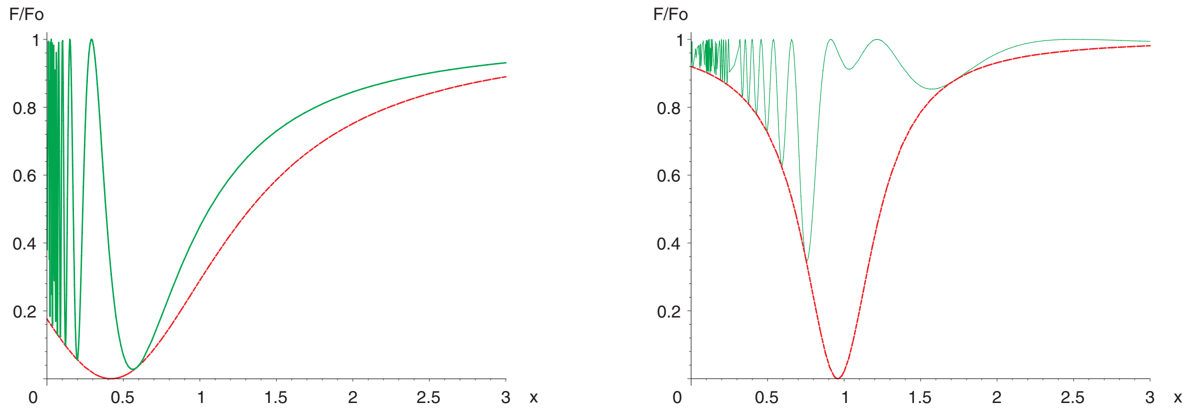

Figure 2. Resonance enhancement of oscillations in matter with constant density. Shown is a dependence of the ratio of the final and original fluxes, F/F_0, on energy ($x \propto E$) for a thin layer, $L = l_0/\pi$ (left panel) and thick layer $L = 10 l_0/\pi$ (right panel). l_0 is the refraction length. The vacuum mixing equals $\sin^2 2\theta = 0.824$.

we show dependence of the ratio $F(E)/F_0(E)$ on energy for thin and thick layers. The oscillatory curve is inscribed in to the resonance curve $(1 - \sin^2 2\theta_m)$. The frequency of the oscillations increases with the length L. At the resonance energy, the oscillations proceed with maximal depths. Oscillations are enhanced in the resonance range:

$$E = E_R \pm \Delta E_R, \quad \Delta E_R = \tan 2\theta \ E_R = \sin 2\theta \ E_R^0, \tag{34}$$

where $E_R^0 = \Delta m^2/2\sqrt{2}G_F n_e$. Notice that for $E \gg E_R$, matter suppresses the oscillation depth; for small mixing the resonance layer is narrow, and the oscillation length in the resonance is large. With increase of the vacuum mixing: $E_R \to 0$ and $\Delta E_R \to E_R^0$.

The oscillations in medium with nearly constant density are realized for neutrinos of different origins crossing the mantle of the Earth.

3.6. MSW: adiabatic conversion
In non-uniform medium, density changes on the way of neutrinos: $n_e = n_e(t)$. Correspondingly, the Hamiltonian of system depends on time, $H = H(t)$, and therefore,

(i) the mixing angle changes during propagation: $\theta_m = \theta_m(n_e(t))$;

(ii) the (instantaneous) eigenstates of the Hamiltonian, ν_{1m} and ν_{2m}, are no more the "eigenstates" of propagation: the transitions $\nu_{1m} \leftrightarrow \nu_{2m}$ occur.

However, if the density changes slowly enough the transitions $\nu_{1m} \leftrightarrow \nu_{2m}$ can be neglected. This is the essence of the adiabatic condition: ν_{1m} and ν_{2m} propagate independently, as in vacuum or uniform medium.

Evolution equation for the eigenstates. Adiabaticity. Let us consider the adiabaticity condition. If external conditions (density) change slowly, the system (mixed neutrinos) has time to adjust this change.

To formulate this condition let us consider the evolution equation for the eigenstate of the Hamiltonian in matter. Inserting $\nu_f = U(\theta_m)\nu_m$ in to equation for the flavor states (22) we obtain

$$i\frac{d\nu_m}{dt} = \begin{pmatrix} H_{1m} & -i\dot{\theta} \\ i\dot{\theta} & H_{2m} \end{pmatrix} \nu_m. \tag{35}$$

As follows from this equation for the neutrino eigenstates [6, 9], $|\dot{\theta}_m|$ determines the energy of transition $\nu_{1m} \leftrightarrow \nu_{2m}$ and $|H_{2m} - H_{1m}|$ gives the energy gap between levels.

If [9]

$$\gamma = \left| \frac{\dot{\theta}_m}{H_{2m} - H_{1m}} \right| \ll 1, \tag{36}$$

the off-diagonal terms can be neglected and equations of the eigenstates split. The condition (36) means that the transitions $\nu_{1m} \leftrightarrow \nu_{2m}$ can be neglected and the eigenstates propagate independently.

For small mixing angles the adiabaticity condition is crucial in the resonance layer where (i) the level splitting is small and (ii) the mixing angle changes rapidly. If the vacuum mixing is small, the adiabaticity is critical in the resonance point. It takes the form [6]

$$\Delta r_R > l_R, \tag{37}$$

where $l_R = l_\nu / \sin 2\theta$ is the oscillation length in resonance, and $\Delta r_R = n_R/(dn_e/dr)_R \tan 2\theta$ is the spatial width of resonance layer.

MSW- effect. Dynamical features of the adiabatic evolution can be summarized in the following way:

- The flavors of the eigenstates change according to density change. The flavor composition of the eigenstates is determined by $\theta_m(t)$.
- The admixtures of the eigenstates in a propagating neutrino state do not change (adiabaticity: no $\nu_{1m} \leftrightarrow \nu_{2m}$ transitions). The admixtures are given by the mixing in production point, θ_m^0.
- The phase difference increases; the phase velocity is determined by the level splitting (which in turn, changes with density (time)).

Now two degrees of freedom become operative: the relative phase and the flavors of neutrino eigenstates. The MSW effect is driven by the change of flavors of the neutrino eigenstates in matter with varying density. The change of phase produces the oscillation effect on the top of the adiabatic conversion.

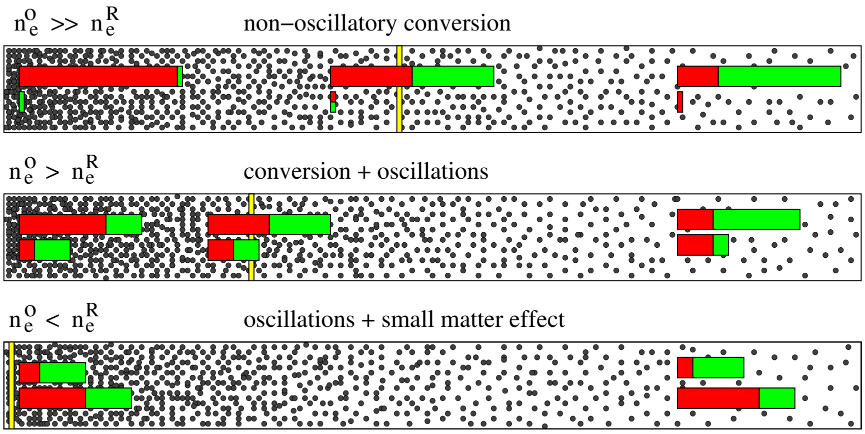

Figure 3. Adiabatic evolution of neutrino state for three different initial condition (n_e^0). Shown are the neutrino states in different moments of propagation in medium with varying (decreasing) density. The yellow vertical line indicates position of resonance. The initial state is ν_e in all the cases. The sizes of the boxes do not change, whereas the flavors (colors) follow the density change.

Let us derive the adiabatic formula [6, 8, 10, 11]. Suppose in the initial moment the state ν_e is produced in matter with density n_0. Then the neutrino state can be written in terms of the eigenstates in matter as

$$\nu_i = \nu_e = \cos\theta_m^0 \nu_{1m} + \sin\theta_m^0 \nu_{2m}, \tag{38}$$

where $\theta_m^0 = \theta_m(n_0)$ is the mixing angle in matter in the production point. Suppose this state propagates adiabatically to the region with zero density (as it happens in the case of the Sun). Then, the adiabatic evolution will consists of transitions $\nu_{1m} \to \nu_1$, $\nu_{2m} \to \nu_2$, and no transition between the eigenstates occurs, so the admixtures are conserved. As a result the final state is

$$\nu_t = \cos\theta_m^0 \nu_1 + \sin\theta_m^0 \nu_2 e^{i\phi}, \tag{39}$$

where ϕ is the adiabatic phase. The survival probability is then given by

$$P = |\langle\nu_e|\nu_t\rangle|^2. \tag{40}$$

Plugging ν_t (39) and ν_e given by (4) into this expression and performing averaging over the phase which means that the contributions from ν_1 and ν_2 add incoherently, we obtain

$$P = (\cos\theta\cos\theta_m^0)^2 + (\sin\theta\sin\theta_m^0)^2 = \sin^2\theta + \cos 2\theta\cos^2\theta_m^0. \tag{41}$$

This formula gives description of the solar neutrino conversion with accuracy 10^{-7} - corrections due to adiabaticity violation are extremely small [12].

Physical picture of the adiabatic conversion. According to the dynamical conditions, the admixtures of eigenstates are determined by the mixing in neutrino production point. This mixing in turn, depends on the density in the initial point, n_e^0, as compared to the resonance density. Consequently, a picture of the conversion depends on how far from the resonance layer (in the density scale) a neutrino is produced.

Three possibilities relevant for solar neutrino conversion are shown in fig. 3. The state produced as ν_e propagates from large density region to zero density. Due to adiabaticity the sizes of boxes which correspond to the neutrino eigenstates do not change.

1). $n_e^0 \gg n_e^R$ - production far above the resonance (the upper panel). The initial mixing is strongly suppressed, consequently, the neutrino state, ν_e, consists mainly of one (ν_{2m}) eigenstate, and furthermore, one flavor dominates in a given eigenstate. In the resonance (its position is marked by the yellow line) the mixing is maximal: both flavors are present equally. Since the admixture of the second eigenstate is very small, oscillations (interference effects) are strongly suppressed. So, here we deal with the non-oscillatory flavor transition when the flavor of whole state (which nearly coincides with ν_{2m}) follows the density change. At zero density we have $\nu_{2m} = \nu_2$, and therefore the probability to find the electron neutrino (survival probability) equals

$$P = |\langle \nu_e | \nu(t) \rangle|^2 \approx |\langle \nu_e | \nu_{2m}(t) \rangle|^2 = |\langle \nu_e | \nu_2 \rangle|^2 \approx \sin^2 \theta. \tag{42}$$

This result corresponds to $\theta_m^0 = \pi/4$ in formula (41).

The value of final probability, $\sin^2 \theta$, is the feature of the non-oscillatory transition. Deviation from this value indicates a presence of oscillations.

2). $n_e^0 > n_e^R$ production above the resonance (middle panel). The initial mixing is not suppressed. Although ν_{2m} is the main component, the second eigenstate, ν_{1m}, has appreciable admixture; the flavor mixing in the neutrino eigenstates is significant. So, the interference effect is not suppressed. As a result, here an interplay of the adiabatic conversion and occurs.

3). $n_e^0 < n_e^R$: production below the resonance (lower panel). There is no crossing of the resonance region. In this case the matter effect gives only corrections to the vacuum oscillation picture.

The resonance density is inversely proportional to the neutrino energy: $n_e^R \propto 1/E$. So, for the same density profile, the condition 1) is realized for high energies, regime 2) for intermediate energies and 3) – for low energies. As we will see all three case are realized for solar neutrinos.

The adiabatic transformations show universality: The averaged probability and the depth of oscillations in a given moment of propagation are determined by the density in a given point and by initial condition (initial density and flavor). They do not depend on density distribution between the initial and final points. In contrast, the phase of oscillations is an integral effect of previous evolution and it depends on a density distribution.

Universal character of the adiabatic conversion can be further generalized in terms of variable [6]

$$n = \frac{n_e^R - n_e}{\Delta n_e^R} \tag{43}$$

which is the distance (in the density scale) from the resonance density in the units of the width of resonance layer. In terms of n the conversion pattern depend only on initial value n_0.

In fig. 4 we show dependences of the average probability and depth of oscillations, that is, $\bar{P}$, P^{max}, and P^{min}, on n. The probability itself is the oscillatory function which is inscribed into the band shown by solid lines. The average probability is shown by the dashed line. The curves are determined by initial value n_0 only, in particular, there is no explicit dependence on the vacuum mixing angle. The resonance is at $n = 0$ and the resonance layer is given by the interval $n = -1 \div 1$. The figure corresponds to $n_0 = -5$, *i.e.*, to production above the resonance layer; the oscillation depth is relatively small. With further decrease of n_0, the oscillation band becomes narrower approaching the line of non-oscillatory conversion. For zero final density we have

$$n_f = \frac{1}{\tan 2\theta}. \tag{44}$$

So, the vacuum mixing enters final condition. For the best fit LMA point, $n_f = 0.45 - 0.50$, and the evolution should stop at this point. The smaller mixing the larger final n_f and the stronger transition.

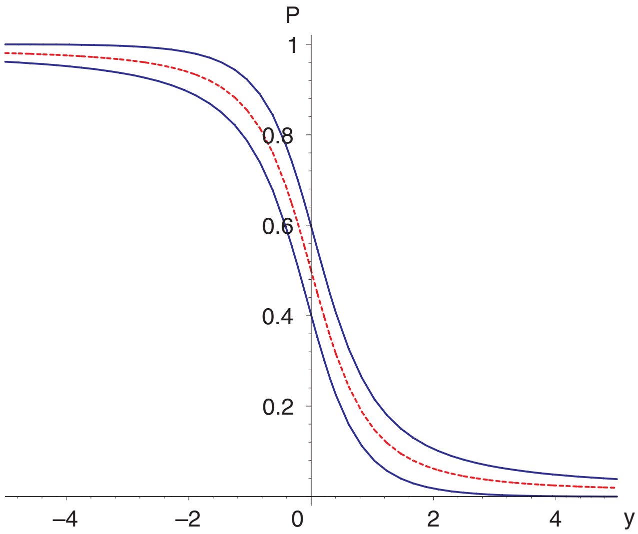

Figure 4. The dependence of the average probability (dashed line) and the depth of oscillations (P^{max}, P^{min} solid lines) on n for $n_0 = -5$. The resonance layer corresponds to $n = 0$. For $\tan^2\theta = 0.4$ (large mixing MSW solution) the evolution stops at $n_f = 0.47$.

3.7. Adiabaticity violation

In the adiabatic regime the probability of transition between the eigenstates is exponentially suppressed $P_{12} \sim exp(-\pi/2\gamma)$ and γ is given in (36) [11, 10]. One can consider such a transition as penetration through a barrier of the height $H_{2m} - H_{1m}$ by a system with the kinetic energy $d\theta_m/dt$.

If density changes rapidly, so that the condition (36) is not satisfied, the transitions $\nu_{1m} \leftrightarrow \nu_{2m}$ become efficient. Therefore admixtures of the eigenstates in a given propagating state change. In our pictorial representation (fig. 5) the sizes of boxes change. Now all three degrees of freedom of the system become operative.

Typically, adiabaticity breaking leads to weakening of the flavor transition. The non-adiabatic transitions can be realized inside supernovas for the very small 1-3 mixing.

4. Determination of the oscillation parameters

4.1. Solar neutrinos

Analysis includes results from the Homestake experiment [13], from Kamiokande and SuperKamiokande [14], from radiochemical Gallium experiments SAGE [15], Gallex [16] and GNO [17] and from SNO [18]. The information we have collected can be described in three-dimensional space:

1. Type of events: νe scattering (SK, SNO), CC-events (Cl, Ga, SNO) and NC events (SNO).

2. Energy of events: radiochemical experiments integrate effect over the energy from the threshold to the maximal energy in the spectrum. Also NC events are integrated over energies. The CC events in SNO and νe events at SuperKamiokande give information about the energy spectrum of original neutrinos.

3. Time dependence of rates (searches for time variation of the flux).

Evidence of conversion. There are three types of observations which testify for the neutrino conversion:

1). Deficit of signal which implies the deficit of the electron neutrino flux. It can be described by the ratio $R \equiv N^{obs}/N^{SSM}$, where N^{SSM} is the signal predicted according to the Standard solar model fluxes [19]. The deficit has been found in all (but SNO neutral current) experiments.

2). Energy spectrum distortion - dependence of the suppression factor on energy. Indirect evidence is provided by comparison of the deficits in experiments sensitive to different energy intervals:

$$Low\ energies\ (Ga) \quad : \quad R = 0.5 - 0.6 \tag{45}$$

$$High\ energies\ (Cl,\ SK,\ SNO) : \quad R \approx 0.3. \tag{46}$$

So the deficit increases with neutrino energy.

3). Smallness of ratio of signals due to charged currents and neutral currents [18]:

$$\frac{CC}{NC} = 0.340 \pm 0.023\ (stat.)\ {}^{+0.029}_{-0.031}(syst.)\ . \tag{47}$$

The latter is considered as the direct evidence of the flavor conversion since NC events are not affected by this conversion, whereas the number CC events is suppressed.

All this testifies for the LMA MSW solution.

Till now there is no statistically significant observations of other signatures of the conversion, namely,

- distortion of the boron neutrino spectrum: up turn at low energies in SK and SNO; (significant effect should be seen below 5 MeV);
- day-night effect (recall that SK agrees with predictions however significance is about 1σ);
- time variations (semiannual) on the top of annual variations (due to eccentricity of the Earth orbit.

Physics of conversion [20]. Physics can be described in terms of three effects

1). Adiabatic conversion (inside the Sun);

2). Loss of coherence of the neutrino state (on the way to the Earth);

3). Oscillations of the neutrino mass states in the matter of the Earth.

According to LMA, inside the Sun the initially produced electron neutrinos undergo the highly adiabatic conversion: $\nu_e \to \cos\theta_m^0 \nu_1 + \sin\theta_m^0 \nu_2$, where θ_m^0 is the mixing angle in the production point. On the way from the central parts of the Sun the coherence of neutrino state is lost after several hundreds oscillation lengths [20], and incoherent fluxes of the mass states ν_1 and ν_2 arrive at the surface of the Earth. In the matter of the Earth ν_1 and ν_2 oscillate partially regenerating the ν_e-flux. With regeneration effects included the averaged survival probability can be written as

$$P = \sin^2\theta + \cos^2\theta_{12}^{m0}\cos 2\theta_{12} - \cos 2\theta_{12}^{m0} f_{reg}. \tag{48}$$

Here the first term corresponds to the non-oscillatory transition (dominates at the high energies), the second term is the contribution from the averaged oscillations which increases with decrease of energy, and the third term is the regeneration effect f_{reg}. At low energies P reduces to the vacuum oscillation probability with very small matter corrections.

Inside the Earth. Entering the Earth the state ν_2 (which dominates at high energies) splits in two matter eigenstates:

$$\nu_2 \to \cos\theta'_m \nu_{2m} + \sin\theta'_m \nu_{1m}. \tag{49}$$

It oscillates regenerating partly the ν_e-flux. In the approximation of constant density profile the regeneration factor equals

$$f_{reg} = 0.5\sin^2 2\theta\ \frac{l_\nu}{l_0}\ . \tag{50}$$

Notice that the oscillations of ν_2 are pure matter effect and for the presently favored value of Δm^2 this effect is small. According to (50), $f_{reg} \propto 1/\Delta m^2$ and the expected day-night asymmetry of the charged current signal equals

$$A_{DN} = f_{reg}/P \sim (3-5)\% \ . \tag{51}$$

Apparently the Earth density profile is not constant and it consists of several layers with slow density change and jumps of density on the borders between layers. It happens that for solar neutrinos one can get simple analytical result for oscillation probability for realistic density profile. Indeed, the solar neutrino oscillations occur in the so called low energy regime when

$$\epsilon \equiv \frac{2EV(x)}{\Delta m^2} \ll 1, \tag{52}$$

which means that the potential energy is much smaller than the kinetic energy. For the LMA oscillation parameters and the solar neutrinos: $\epsilon(x) = (1-3) \cdot 10^{-2}$. In this case one can use small parameter $\epsilon(x)$ (52) to develop the perturbation theory [21]. The following expression for the regeneration factor

$$f_{reg} = \frac{1}{2}\sin^2 2\theta \int_{x_0}^{x_f} dx V(x) \sin\phi_m(x \to x_f). \tag{53}$$

Here x_0 and x_f are the initial and final points of propagation correspondingly, and $\phi_m(x \to x_f)$ is the adiabatic phase acquired between a given point of trajectory, x, and final point, x_f. The latter feature has important consequence leading to the attenuation effect - weak sensitivity to the remote structures of the density profile when non-zero energy resolution of detector is taken into account.

Another insight into phenomena can be obtained using the adiabatic perturbation theory which leads to [12]

$$f_{reg} = \frac{2E\sin^2 2\theta}{\Delta m^2} \sin\frac{\phi_0}{2} \sum_{j=0...n-1} \Delta V_j \sin\frac{\phi_j}{2}. \tag{54}$$

Here ϕ_0 and ϕ_j are the phases acquired along whole trajectory and on the part of the trajectory inside the borders j. This formula corresponds to symmetric profile with respect to the center of trajectory. Using (54) one can easily infer the attenuation effect. The formula reproduces precisely the results of exact numerical calculations.

4.2. KamLAND

KamLAND (Kamioka Large Anti-neutrino detector) is the reactor long baseline experiment [22] . Few relevant details: 1kton liquid scintillator detector situated in the Kamioka laboratory detects the antineutrinos from surrounding atomic reactors (about 53) with the effective distance (150 - 210) km. The classical reaction of the inverse beta decay, $\bar{\nu}_e p \to e^+ n$, is used. The data include

(i) the total rate of events;

(ii) the energy spectrum (fig. 5);

(iii) the time dependence of the signal which is due to variations of the reactors power. (Establishing the correlation between the neutrino signal and power of reactors is important check of the whole experiment). In fact, this change also influences the oscillation effect since the effective distance from the reactors changes (*e.g.*, when power of the closest reactor decreases).

In the oscillation analysis the energy threshold $E > 2.6$ eV is established.

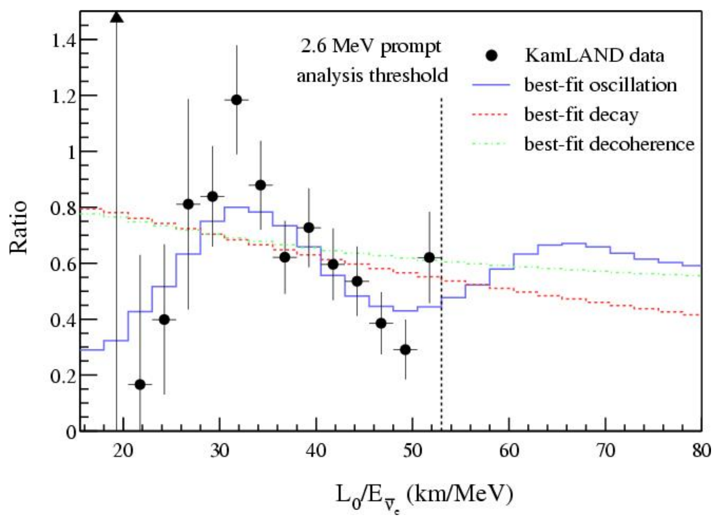

Figure 5. The L/E distribution of events in the KamLAND experiment; from [22].

The physics process is essentially the vacuum oscillations of $\bar{\nu}_e$. The matter effect, about 1%, is negligible at the present level of accuracy.

The evidences of the oscillations are

1). The deficit of the number of the $\bar{\nu}_e$ events

$$R_\nu = \frac{N_{obs}}{N_{expect}} = \frac{258}{365.2 \pm 23.7} \sim 0.7 \tag{55}$$

for $E > 2.6$ MeV.

2). The distortion of the energy spectrum or L/E dependence (when some reactors switch off the effective distance changes). Notice the absence of strong spectrum distortion excludes large part of the parameter space Δm^2.

Comparison of results from the solar neutrinos and KamLAND open important possibility to check the theory of neutrino oscillation and conversion test CPT, search for new neutrino interactions and new neutrino states.

4.3. Atmospheric neutrinos

Experimental results. The atmospheric neutrino flux is produced in interactions of the high energy cosmic rays (protons, nuclei) with nuclei of atmosphere. The interactions occur at heights (10 - 20) km. At low energies the flux is formed in the chain of decays: $\pi \to \mu\nu_\mu$, $\mu \to e\nu_e\nu_\mu$. So, each chain produces $2\nu_\mu$ and $1\nu_e$, and correspondingly, the ratio of fluxes equals

$$r \equiv \frac{F_\mu}{F_e} \approx 2. \tag{56}$$

With increase of energy the ratio increases since the lifetime acquires the Lorentz boost and muons have no time to decay before collisions: they are absorbed or loose the energy. As a consequence, the flux of the electron neutrinos decreases.

In spite of the long term efforts, the predicted atmospheric neutrino fluxes have still large uncertainties (about 20% in overall normalization and about 5% in the so called “tilt” parameter which describes the uncertainty in energy dependence of the flux). The origin of uncertainties is twofold: original flux of the cosmic rays and cross sections of interactions.

The recent analyses include the data from Baksan telescope, SuperKamiokande [23], MACRO [24], SOUDAN [25]. The data can be presented in the three dimensional space which includes

- type of events detected: e-like events (showers), μ-like events, multi-ring events, NC events (with detection of π^0), τ enriched events.

- energy of events: widely spread classification includes the sub-GeV and multi-GeV events, stopping muons, through-going muons, *etc.*.

- zenith angle (upward going, down going, *etc*).

Now MINOS experiment [26] provides with some early information on effects for neutrinos and antineutrinos separately.

The evidence of the atmospheric neutrino oscillations includes:

1). Smallness of the double ratio of numbers of μ-like to e-like events [23]:

$$R_{\mu/e} \equiv \frac{N_\mu^{obs}/N_\mu^{th}}{N_e^{obs}/N_e^{th}}. \tag{57}$$

The ratio weakly depends on energy. Apparently in the absence of oscillations (or other non-standard neutrino processes) the double ratio should be 1. The smallness of the ratio testifies for disappearance of the ν_μ flux.

2). Distortion of the zenith angle dependence of the μ -like events.

The up-down asymmetry is defined as

$$A_{up/down} \equiv \frac{N_{up}}{N_{down}}. \tag{58}$$

Due to complete up-down symmetric configuration for the production, in the absence of oscillations or other non-standard effect the asymmetry should be absent: $A_{up/down} = 1$.

Substantial distortion of the zenith angle distribution is found. The deficit of numbers of events which increases with decrease of $\cos\theta_Z$ and reaches about 1/2 in the upgoing vertical direction for multi-GeV events. The distortion increases with energy. That is, the up-down asymmetry increases with energy:

In contrast to the μ-like, the e-like events distribution does not show any anomaly. Though one can mark some excess (about 15%) of the e-like events in the sub-GeV range.

3). Appearance of the τ-like events [23].

4). L/E dependence shows the first oscillation minimum (fig. 6).

In the first approximation all these data can be consistently described in terms of the $\nu_\mu - \nu_\tau$ vacuum oscillations. Notice that for pure 2ν oscillations of this type no matter effect is expected: the matter potentials of the ν_μ and ν_τ are equal. In the context of three neutrino mixing, for non-zero values of $\sin\theta_{13}$ the matter effect should be taken into account for the $\nu_\mu - \nu_\tau$ channel

Notice that unique description is valid for different types of events and in a very wide range of energies: from 0.1 to more than 100 GeV.

4.4. K2K

The $\nu_\mu-$ beam with typical energies $E = (0.5-3)$ GeV created at KEK was directed to Kamioka and its interations were detected at SuperKamiokande [30]. The baseline (the source-detector distance) is about 250 km. The oscillations of muon neutrinos, $\nu_\mu \to \nu_\mu$, (as well as $\nu_\mu \to \nu_e$ - transition probability) have been studied by comparison of the detected number of μ-like events and the energy spectrum with the predicted ones. The predictions have been made by extrapolating of the results from the "front" detector to the SK place. The front detector similar to SK

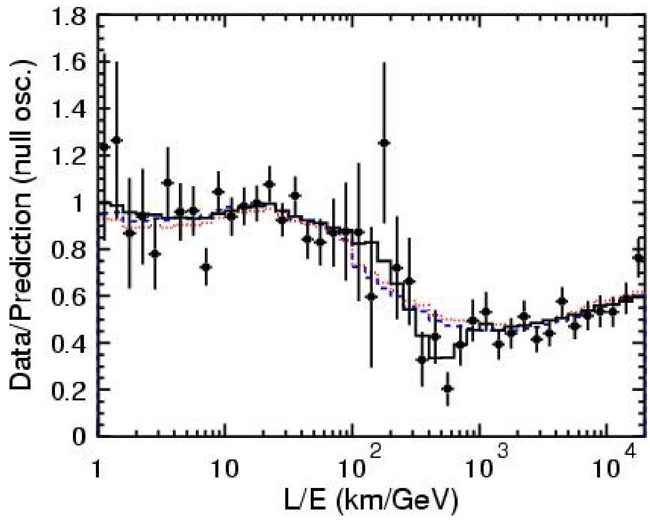

Figure 6. L/E distribution of the atmospheric μ like events; from [27]

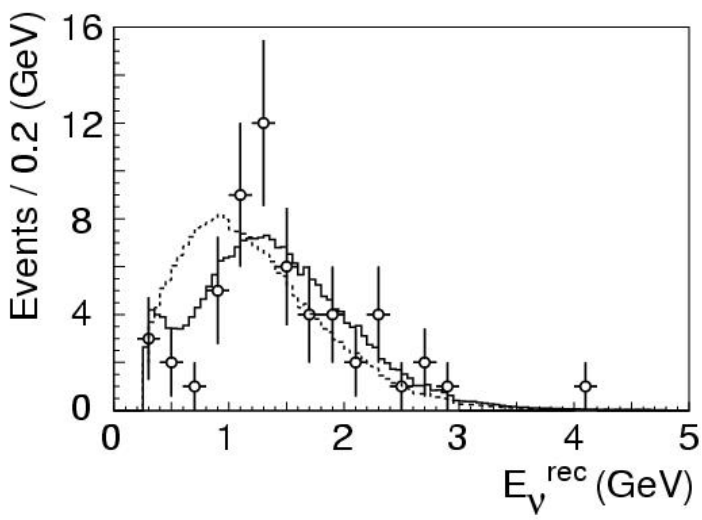

Figure 7. The energy spectrum of events in the K2K experiment, from [30].

(but of smaller scale) was at about 1 km distance from the source and detected the μ-like events.

The evidence of oscillations was (i) the deficit of the total number of events: 107 events have been observed whereas 151^{+12}_{-10} have been expected. (ii) The spectrum distortion has been found (fig. 7).

The data are interpreted as the non averaged vacuum oscillations $\nu_\mu - \nu_\tau$.

The energy distribution of the detected μ -like events gives an evidence of the first oscillation dip at $E \sim 0.5$ GeV (see fig. 7).

4.5. 1-3 mixing: effects and bounds

θ_{13} is the last unknown angle in the mixing matrix of active neutrinos;

θ_{13} has important phenomenological consequences: it can produce leading effects for supernova

electron (anti) neutrinos and sub-leading effects in the solar and atmospheric neutrinos;
θ_{13} controls the CP-violation in the leptonic sector;
θ_{13} produces the sub-leading effects in the neutrino mass matrix in the flavor basis;
as we will see θ_{13} provides crucial test of mechanism of the lepton mixing enhancement;
non-zero values of θ_{13} can be related to (flavor?) symmetry breaking in the leptonic sector, thus providing tests of this violation.

The direct bounds on 1-3 mixing are obtained in the CHOOZ experiment [31]. This is the experiment with a single reactor and single detector with baseline about 1 km. The effect is vacuum non-average oscillations with survival probability given by the standard oscillation formula

$$P = 1 - \sin^2 2\theta_{13} \sin^2 \phi/2. \tag{59}$$

The baseline is comparable with the half oscillation length: For the bf value of Δm^2 from the atmospheric neutrino studies at $E \sim 2$ MeV the oscillation length equals ~ 2 km.

The signature of the oscillations consists of distortion of the energy spectrum described by (59). No distortion has been found within the error bars.

4.6. Global fits

In fig. 8 we show the results of the global fit of the oscillation data performed in [29].

Results of global fits of the other groups (see [32]) agree very well. Different types of experiments confirm each other: KamLAND confirms solar neutrino results, K2K - the atmospheric neutrino results *etc.*. Furthermore, unique interpretation of whole bulk of the data in terms of vacuum masses and mixings provides with the overall confirmation of the picture So, the determination of the parameters is rather robust, and it is rather non-plausible that future measurements will lead to significant change.

The most probable values of parameters equal

$$\Delta m_{12}^2 = (7.9 - 8.0) \cdot 10^{-5} \ \ \text{eV}^2, \tag{60}$$

$$\sin^2 \theta_{12} = 0.310 - 0.315, \tag{61}$$

$$\Delta m_{23}^2 = (2.4 - 2.5) \cdot 10^{-3} \ \ \text{eV}^2 \tag{62}$$

$$\sin^2 \theta_{23} = 0.44 - 0.50. \tag{63}$$

The parameter which describes the deviation of the 23 mixing from maximal equals

$$D_{23} \equiv 0.5 - \sin^2 \theta_{23} = 0.03 - 0.06. \tag{64}$$

For 1-3 mixing we have

$$\sin^2 \theta_{23} = 0.00 - 0.01, \qquad 1\sigma = 0.011 - 0.013. \tag{65}$$

Table 2. Experiments and relevant oscillation parameters.

Experiments	parameters of leading effects	parameters of sub-leading effects
Solar neutrinos, KamLAND	Δm_{12}^2, θ_{12}	θ_{13}
Atmospheric neutrinos	Δm_{23}^2, θ_{23}	Δm_{12}^2, θ_{12}, θ_{13}, δ
K2K	Δm_{23}^2, θ_{23}	θ_{13}
CHOOZ	Δm_{23}^2, θ_{13}	strongly suppressed
MINOS	Δm_{23}^2, θ_{23}	θ_{13}

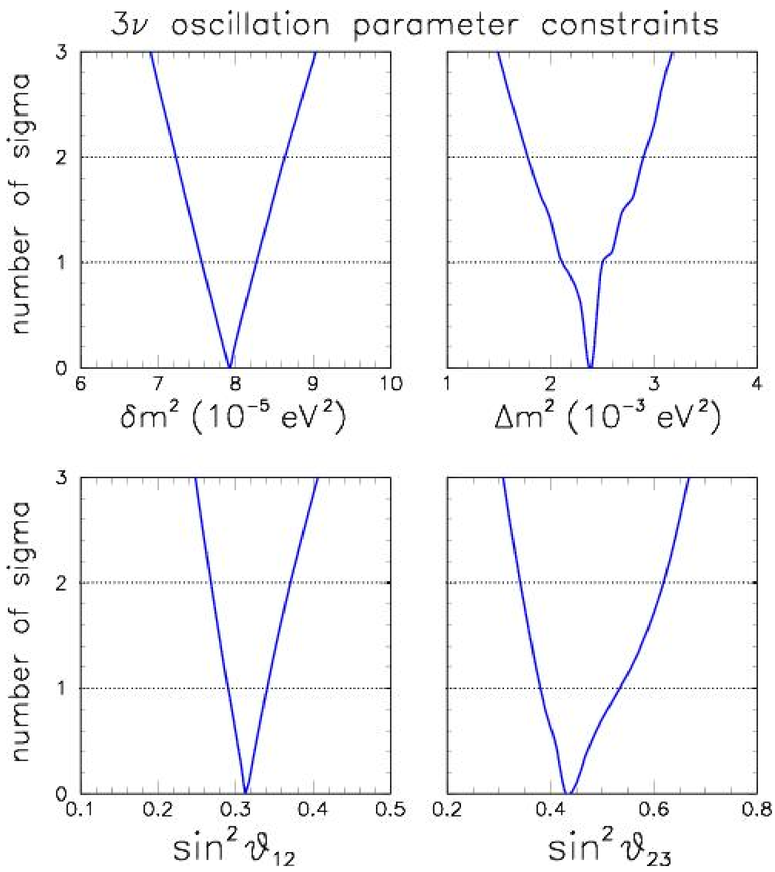

Figure 8. The results of global 3ν analysis for 1-2 and 2-3 mass splits and mixings; from [29].

The ratio of mass squared differences important for theoretical implications equals

$$r_\Delta \equiv \frac{\Delta m_{12}^2}{\Delta m_{23}^2} = 0.031 - 0.033. \tag{66}$$

5. Neutrino mass and flavor spectrum

5.1. Spectrum

Information obtained from the oscillation experiments allows us to make significant progress in reconstruction of the neutrino mass and flavor spectrum (Fig. 9).

The unknowns are:

(i) admixture of ν_e in ν_3, U_{e3};

(ii) type of mass spectrum: hierarchical, non-hierarchical with certain ordering, degenerate, which is related to the value of the absolute mass scale, m_1;

(iii) type of mass hierarchy (ordering): normal, inverted (partially degenerate);

(iv) CP-violation phase δ.

Information described in the previous sections can be summarized in the following way.

1. The observed ratio of the mass squared differences (66) implies that there is no strong hierarchy of neutrino masses:

$$\frac{m_2}{m_3} > \sqrt{\frac{\Delta m_{12}^2}{\Delta m_{23}^2}} = 0.18 \pm 0.02. \tag{67}$$

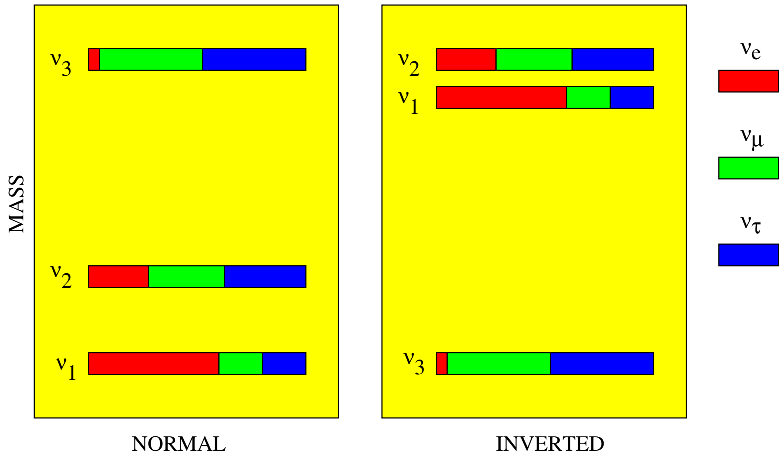

Figure 9. Neutrino mass and flavor spectra for the normal (left) and inverted (right) mass hierarchies. The distribution of flavors (colored parts of boxes) in the mass eigenstates corresponds to the best-fit values of mixing parameters and $\sin^2\theta_{13} = 0.05$.

For charge leptons the corresponding ratio is 0.06, and even stronger hierarchies are observed in the quark sector.

2. There is the bi-large or large-maximal mixing between the neighboring families (1 - 2) and (2 - 3). Still rather significant deviation of the 2-3 mixing from the maximal one is possible.

3. Mixing between remote (1-3) families is weak.

5.2. Absolute scale of neutrino mass

Direct kinematic methods - measurements of the Curie plot of the ^3H decay near the end point - give $m_e < 2.05$ eV (95%), Troitsk after "anomaly" subtraction [33]. And the updated in 2004 result from Mainz experiment [34] $m_e < 2.3$ eV (95%). Future KATRIN experiment [35] aims at one order of magnitude better upper bound: $m_e < 0.2$ eV (90%). The discovery potential is estimated so that the positive result $m_e = 0.35$ eV can be established at 5σ (statistical) level.

From oscillation experiments we get the lower bound on mass of the heaviest neutrino:

$$m_h > \sqrt{\Delta m^2_{atm}} = 0.04 \text{ eV} \quad (95\%). \tag{68}$$

In the case of normal mass hierarchy $m_h = m_3$ and in the inverted hierarchy case $m_h = m_1 \approx m_2$.

5.3. Neutrinoless double beta decay

Results. The rate neutrinoless double beta decay is determined by effective Majorana mass of electron neutrino

$$m_{ee} = \left| \sum_k U^2_{ek} m_k e^{i\phi(k)} \right| , \tag{69}$$

$\Gamma \propto m^2_{ee}$. Here $\phi(k)$ is the phase of the k eigenvalue.

The best present bound on m_{ee} is given by the Heidelberg-Moscow experiment: $m_{ee} < 0.35 - 0.50$ eV [36]. Part of collaboration claims evidence of a positive signal [37, 38]. Some details follow.

The Heidelberg-Moscow collaboration searched for the mode of the decay

$$^{76}Ge \rightarrow ^{76}Se + e^- + e^- \tag{70}$$

with the end point $Q_{ee} = 2039$ keV. The total statistics collected from 5 enriched Ge detectors is 71.7 kg yr. The peak at the end point of spectrum has been found and interpreted in [38] as due to neutrinoless double beta decay.

There is a number of arguments *pro and contra* of such interpretation.

Number of events in the peak (interpreted as $\beta\beta_{0\nu}$ decay gives the half-lifetime

$$T_{1/2} = 1.19 \cdot 10^{25} \text{ y}, \quad 3\sigma \text{ range} : (0.69 - 4.18) \cdot 10^{25} \text{ y}. \tag{71}$$

The significance of the peak depends on model of background and quoted by the authors as 4.2σ.

If the exchange of light Majorana neutrino is the dominant mechanism of decay, the measured life time corresponds to the effective mass of the Majorana neutrino:

$$m_{ee} = 0.44 \text{ eV}, \quad 3\sigma \text{ range} : (0.24 - 0.58) \text{ eV}. \tag{72}$$

Other groups do not see signal of the $\beta\beta_{0\nu}$ decay though their sensitivity is somehow lower.

Measurements of the neutrinoless double beta decay are of the fundamental importance: apart from checks of the total lepton number conservation and Majorana nature of neutrinos they can provide information about properties of the neutrino mass spectrum: the absolute mass scale and type of mass hierarchy.

Fig. 10 from [32] summarizes the present knowledge of the absolute mass scale. Shown are the allowed (by oscillation measurements) regions in the $m_{ee} - m_l$-plane, where m_l is lightest neutrino probed by the direct kinematical methods and cosmology.

There are several benchmark values of m_{ee}. Apparently if the Heidelberg-Moscow positive result is confirmed, and if it is due the light Majorana neutrino mass, the neutrino mass spectrum should be quasidegenerate.

1). The bound $m_{ee} < 0.05$ eV will exclude the degenerate spectrum;

2). The bound $m_{ee} < 0.01$ eV will exclude the inverted hierarchy.

3). For the plausible scenario with normal mass hierarchy one expects $m_{ee} = 0.003 \pm 0.002$ eV.

4). Strong cancellation, $m_{ee} < 0.001$ eV, is expected for $m_1 = 0.002 - 0.008$ eV.

5.4. Cosmology and neutrino mass

The best cosmological bound follows from studies of Large scale structure Analysis of the cosmological data which includes CMB, SDSS of galaxies, Lyman alpha forest observations and weak lensing lead to the upper bound [39]

$$m < 0.13, \quad \text{eV}, \quad 95\%. \tag{73}$$

Apparently the positive claim of observation of neutrinoless double beta decay is disfavored by the cosmological data.

In future, the weak lensing will allow to perform direct measurements of clustering of all matter and not just luminous one. This will improve the sensitivity down to $\sum_i m_i \sim 0.03$ eV.

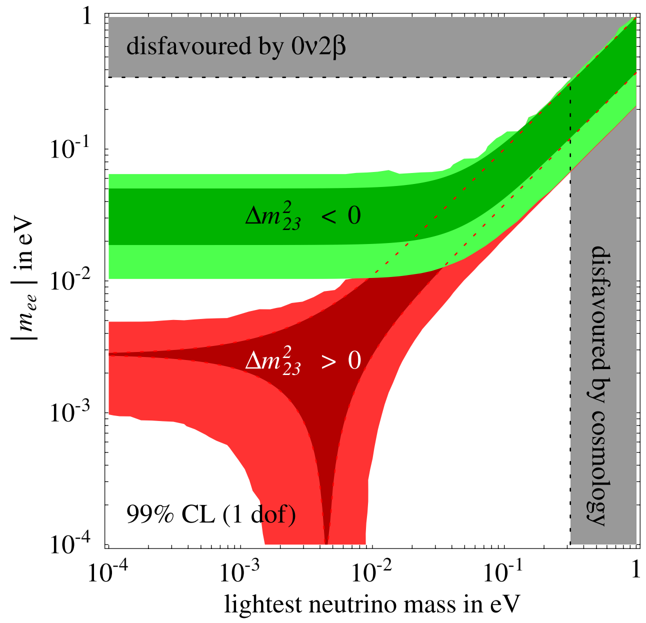

Figure 10. The 90% CL range for m_{ee} as a function of the lightest neutrino mass for the normal ($\Delta m^2_{23} > 0$) and inverted ($\Delta m^2_{23} < 0$) mass hierarchies.[28] The darker regions show how the allowed range for the present best-fit values of the parameters with negligible errors; from [32].

5.5. LSND result and new neutrinos

Large Scintillator Neutrino Detector collaboration studied interactions of neutrinos from Los Alamos Meson Physics Facility. In particular, neutrinos from the decay chain: $\pi^+ \to \mu^+ + \nu_e$, $\mu^+ \to e^+ + \nu_e + \bar{\nu}_\mu$. The excess of the $(e^+ + n)$ events has been observed in the detector which could be due to inverse beta decay: $\bar{\nu}_e + p \to e^+ + n$ [40]. In turn $\bar{\nu}_e$ could appear due to oscillations $\bar{\nu}_\mu - \bar{\nu}_e$ in the original $\bar{\nu}_\mu$ beam. If confirmed the LSND result may substantially change implications of the discussed results.

Interpretation of the excess in terms of the $\bar{\nu}_\mu - \bar{\nu}_e$ oscillations would correspond to the transition probability

$$P = (2.64 \pm 0.76 \pm 0.45) \cdot 10^{-3}. \tag{74}$$

The allowed region is restricted from below by $\Delta m^2 > 0.2$ eV^2.

This result is clearly beyond the "standard 3ν picture. It implies new sector and new symmetries of the theory.

The situation with this ultimate neutrino anomaly [40] is really dramatic: all suggested physical (not related to the LSND methods) solutions are strongly or very strongly disfavored now. At the same time, being confirmed, the oscillation interpretation of the LSND result may change our understanding the neutrino (and in general fermion) masses.

Even very exotic possibilities are disfavored. An analysis performed by the KARMEN collaboration[41] has further disfavored a scenario[42] in which the $\bar{\nu}_e$ appearance is explained by the anomalous muon decay $\mu^+ \to \bar{\nu}_e \bar{\nu}_i e^+$ $(i = e, \mu, \tau)$.

The CPT-violation scheme[43] with different mass spectra of neutrinos and antineutrinos is disfavored by the atmospheric neutrino data [44]. No compatibility of LSND and "all but LSND" data have been found below 3σ [45].

The main problem of the (3 + 1) scheme with $\Delta m^2 \sim 1$ eV^2 is that the predicted LSND signal, which is consistent with the results of other short base-line experiments (BUGEY, CHOOZ, CDHS, CCFR, KARMEN) as well as the atmospheric neutrino data, is too small: the $\bar{\nu}_\mu \to \bar{\nu}_e$ probability is about 3σ below the LSND measurement.

Introduction of the second sterile neutrino with $\Delta m^2 > 8$ eV^2 may help [46]. It was shown[47] that a new neutrino with $\Delta m^2 \sim 22$ eV^2 and mixings $U_{e5} = 0.06$, $U_{\mu 5} = 0.24$ can enhance the predicted LSND signal by (60 − 70)%. The (3 + 2) scheme has, however, problems with cosmology and astrophysics. The combination of the two described solutions, namely the 3 + 1 scheme with CPT-violation has been considered [48].

Some recent proposals including the mass varying neutrinos MaVaN [49] and decay of heavy sterile neutrinos [50] also have certain problems.

MiniBooNE [51] is expected to clarify substantially interpretation of the LSND result. MiniBooNE searches for ν_e appearance in the 12 m diameter tank filled in by the 450 t of mineral oil scintillator and covered by 1280 PMT. The flux of muon neutrinos with the average energy $\langle E_\nu \rangle \approx 800$ MeV is formed in π decays (50m decay pipe) which are in turn produced by 8 GeV protons from the Fermilab Booster. The 541 m baseline is about half of the oscillation length for $\Delta m^2 \sim 2$ eV^2. The results of (blind) oscillation analysis will be published in 2006.

6. Mass and mixing

There are two salient features related to neutrinos:

- smallness of neutrino mass
- peculiar mixing pattern.

It would be natural to assume that both originate from the same mechanism which is, in fact, related to the neutrality of neutrinos. At the same time the situation can be much more complicated - mass and mixing may not be immediately related For instance the mixing pattern can be determined by some particular symmetries which do not determine masses, smallness of neutrino mass and mixing pattern decouple.

6.1. Remarks

Suppose the SM particles are the only light degrees of freedom. Then at low energies (after integrating out the heavy degrees of freedom) one can get the operator: [52]

$$\frac{\lambda_{ij}}{M}(L_i H)^T (L_j H), \quad i, j = e, \mu, \tau, \tag{75}$$

where L_i is the lepton doublet, λ_{ij} are the dimensionless couplings and M is the cut-off scale. After EW symmetry breaking it generates the neutrino masses

$$m_{ij} = \frac{\lambda_{ij}\langle H \rangle^2}{M}. \tag{76}$$

For $\lambda_{ij} \sim 1$ and $M = M_{Pl}$ we find $m_{ij} \sim 10^{-5}$ eV [53]. Several important conclusions follow immediately from this consideration.

The Planck scale (gravitational) interactions are not enough to generate the observed values of the masses. So, new scales of physics below M_{Pl} should exist.

It has been found that contributions to the neutrino masses of the order $\sim 10^{-5}$ eV are still relevant for phenomenology. Furthermore the sub-dominant structures of the mass matrix can be generated by the Planck scale interactions [54]. So, the neutrino mass matrix can get observable contributions from all possible energy/mass scales from the EW scale (or even lower) to the Planck scale. As a consequence, the structure of the mass matrix can be rather complicated.

6.2. Seesaw

The see-saw (type I) mechanism [55, 56] implements the neutrality in full strength (Majorana nature, heavy RH components). Let us introduce the Dirac mass matrix, $m_D = Y v_{EW}$, where Y is the matrix of Yukawa couplings and v_{EM} is the electroweak VEV, and the Majorana mass matrix for the RH neutrinos M. Then in in the basis ν, N, ($N = (\nu_R)^c$) we have the mass matrix

$$\begin{pmatrix} 0 & m_D^T \\ m_D & M \end{pmatrix}. \tag{77}$$

For $m_D \ll M$ the diagonalization gives the mass matrix of light neutrinos

$$m = -m_D^T M_R^{-1} m_D \qquad (type\ I). \tag{78}$$

If the $SU(2)$ triplet, Δ_L, exists which develops a VEV $\langle \Delta_L \rangle$, the left-handed neutrinos can get a direct mass m_L via the interaction $f_\Delta L^T L \Delta_L$. If Δ_L is very heavy, it can develop the induced VEV from interactions with a doublet: $\langle \Delta_L \rangle = v_{EW}^2/M$. So that

$$m_L = f_\Delta \frac{v_{EW}^2}{M} \qquad (type\ II), \tag{79}$$

and here we deal with the see-saw of VEV's [57].

In $SO(10)$ with 126_H-plet of Higgses we have $M_R = f v_R$, where f is the Yukawa coupling of the matter 16-plet with 126_H and v_R is the VEV of the $SU(5)$ singlet component of 126_H. Now $f_\Delta = f$, and the general mass term which contains both types of contributions can be written as

$$m = \frac{v_{EM}^2}{v_R}(f\lambda - Y^T f^{-1} Y). \tag{80}$$

Here λ is the coupling of 10- and 126-plets of Higgses responsible for the induced VEV of triplet in 126. According to this expression the flavor structure of the two contributions may partially correlate.

GU theories provide with a large mass scale comparable to the scale of RH neutrino masses. Furthermore, one can argue that GUT + see-saw can naturally lead to the large lepton mixing in contrast to the quark mixing. or inversely, one can say that the large lepton mixing testifies for Grand Unification. Indeed, suppose that all quarks and leptons of a given family are in a single multiplet F_i (as 16 of SO(10)). Suppose also that all Yukawa couplings are of the same order thus producing matrices with generically large mixing.

If in the first approximation the Dirac masses are generated by an unique Higgs multiplet, say 10_H of SO(10), the mass matrices of the up and down components of the weak doublets have identical structures, and so, will be diagonalized by the same rotations. As a result, no mixing appears for quarks, and masses of up and down components will be equal to each other.

In contrast to other fermions, the RH neutrinos acquire Majorana masses via the additional Yukawa couplings (with 126_H of SO(10)). If those couplings are also of the generic form, they produce M_R with large mixing which leads then to non-zero lepton mixing. So in the lowest approximation the quark mixing is zero and the lepton mixing can be large. Then the quark mixing appears as correction.

The problem of this scenario is the strong hierarchy of the quark and lepton masses. Indeed, taking the neutrino Dirac masses as $m_D \sim diag(m_u, m_c, m_t)$ in a spirit of GU, we find that for generic M_R the see-saw type I formula (78) produces strongly hierarchical mass matrix with small mixings unless M_R has a special structure which compensates the strong hierarchy in m_D.

Other solutions include a substantial difference in the Dirac matrices of quarks and leptons: $m_D(q) \neq m_D(l)$ or a type II see-saw for which there is no relation to m_D. Let us consider the first possibility.

6.3. See-Saw enhancement of mixing

Can the same mechanism (see-saw) which explains the smallness of the neutrino mass also explain the large lepton mixing? The idea is that [58] due to the (approximate) quark-lepton symmetry, the Dirac mass matrices of the quarks and leptons have the same (similar) structure $m_D \sim m_{up}$, $m_l \sim m_{down}$ leading to small mixing in the Dirac sector. The special structure of M_R (which has no analogue in the quark sector) leads to an enhancement of lepton mixing. Two different possibilities have been found [58]:

- strong (nearly quadratic) hierarchy of the RH neutrino masses: $M_{iR} \sim (m_{iup})^2$; and
- strong interfamily connection (pseudo Dirac structures) like

$$M_R \approx \begin{pmatrix} A & 0 & 0 \\ 0 & 0 & B \\ 0 & B & 0 \end{pmatrix}, \quad \text{or} \quad \begin{pmatrix} 0 & A & 0 \\ A & 0 & 0 \\ 0 & 0 & B \end{pmatrix}. \tag{81}$$

(Small corrections should be introduced to these matrices.) In the three neutrino context both possibilities can be realized simultaneously, so that the pseudo Dirac structure leads to maximal 2-3 mixing, whereas the strong hierarchy $A \ll B$ enhances the 1-2 mixing.

6.4. Extra dimensions and neutrino mass

Theories with extra space dimensions provide qualitatively new mechanism of generation of the small *Dirac* neutrino mass. There are different scenarios, however their common feature can be called the overlap suppression: the overlap of wave functions of the left, $\nu_L(y)$, and right , $\nu_R(y)$ handed components in extra dimensions (coordinate y). The suppression occurs due to different localizations of the $\nu_L(y)$ and $\nu_R(y)$ in the extra space. The effective Yukawa coupling is proportional to the overlap. One can introduce also suppression of overlap of neutrinos with Higgs field. Let us consider realizations of the overlap suppression mechanism in different extra dimensional scenarios.

Large flat extra dimensions: ADD scenario. The setup is the $3D$ spatial brane embedded in $(3+\delta)D$ bulk [59]. Extra dimensions have large radii $R_i \gg 1/M_{Pl}$ which allows one to reduce the fundamental scale of theory down to $M^* \sim 10 - 100$ TeV [59]. The left handed neutrino is localized on the brane, whereas the right handed component (being the singlet of the gauge group) propagates in the bulk (see fig. 11a).

To clarify the mechanism of suppression let us consider one extra dimension of radius R. (Generalization to several extra dimensions is straightforward.) Since the RH component is not localized, we find from the normalization condition that its wave function has typical value $\nu_R(y) \sim 1/\sqrt{R}$. The effective width of the brane is of the order $d \sim 1/M^*$, so the amplitude of probability to find the RH neutrino on the brane equals

$$d^{1/2}\nu_R \sim \frac{1}{\sqrt{M^* R}}. \tag{82}$$

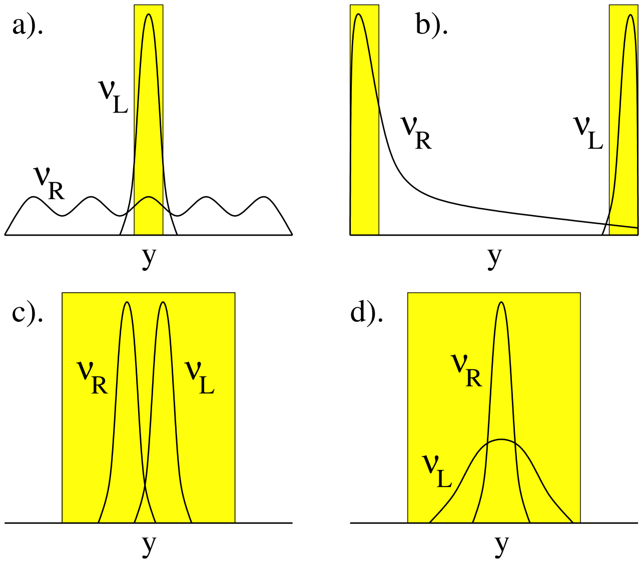

Figure 11. The overlap mechanism of small Dirac neutrino mass generation in models with extra spatial dimensions. a). Large flat extra dimensions. b). Warped extra dimensions. c - d). Models of "fat" branes.

Since the LH neutrino is localized on the brane, this factor describes the overlap of the wave functions.

Generalization to δ extra dimensions is straightforward: for the overlap factor we get

$$\frac{1}{\sqrt{M^{*\delta} V_\delta}}, \tag{83}$$

where V_δ is the volume of extra dimensions. Using the relation between the effective Planck mass and the fundamental mass scale M^*:

$$M_{Pl}^2 = M^{*2+\delta} V_\delta, \tag{84}$$

we can rewrite the overlap factor as

$$\frac{M^*}{M_{Pl}} \tag{85}$$

which does not depend on the number of extra dimensions explicitly. If λ is the Yukawa coupling for neutrinos in the $(4+\delta)D$ theory, the effective coupling in 4D will be suppressed by this overlap factor. Consequently,

$$m_D = \lambda v_{EW} \frac{1}{\sqrt{M^{*\delta} V_\delta}} = \lambda v_{EW} \frac{M^*}{M_{Pl}}. \tag{86}$$

For $M^* \sim 100$ TeV and $\lambda \sim 1$ we obtain from (86) $m_D \sim 10^{-2}$ eV.

Warped extra dimensions: Randall-Sundrum scenario. A set up is one extra dimension compactified on the S^1/Z_2 orbifold, and non-factorizable metric. The coordinate in the extra dimension is parameterized by $r_c\phi$, where r_c is the radius of extra dimension and the angle ϕ changes from 0 to π. Two branes are localized in different points of extra dimension: the "hidden" brane is at $\phi = 0$ and the observable one is at $\phi = \pi$ [60]. The wave function of the RH neutrino $\nu_R(\phi)$ is centered on the hidden brane, whereas the LH one - on the visible brane (see fig. 11 b). Due to warp geometry $\nu_R(\phi)$ exponentially decreases from the hidden to the observable brane. On the observable brane it is given by

$$\nu_R(\pi) \sim \epsilon^{\nu-1/2}, \quad \epsilon = e^{-kr_c\pi} = \frac{v_{EW}}{M_{Pl}}. \tag{87}$$

Here M_{Pl} is the Planck scale, $k \sim M_{Pl}$ is the curvature parameter. In (87) $\nu \equiv m/k$ and $m \sim M_{Pl}$ is the Dirac mass in 5D. Essentially $\nu_R(\pi)$ gives the overlap factor and the Dirac mass on the visible brane equals

$$m_D = \lambda \nu_R(\pi) v_{EW} \sim M \left(\frac{V_{EW}}{M}\right)^{\nu+1/2}. \tag{88}$$

For $\nu = 1.1 - 1.6$ we get the mass in the phenomenologically required range. Notice that expression for the mass is of the seesaw type with, however, arbitrary power of small ratio. Now explanation of smallness of the neutrino mass is reduced to explanation of particular values of the mass m. Small variations of m can produce strong change in the light neutrino masses. Though the mass parameters can be all of the same order their particular values should be fine tuned.

Different realization is when both ν_L and ν_R are on the TeV brane whereas the lepton number is violated on the Planck brane [61].

Fat brane scenarios. The LH and RH neutrino wave functions can be localized differently on the same "fat" brane [62]. There are various possibilities to suppress the overlap:

1). localize ν_L and ν_R in different places of the brane (fig. 11 c);

2). arrange parameters in such a way that the RH neutrino is localized in the narrow region of the fat brane, whereas the LH neutrino wave function is distributed in whole the brane (fig.11d) [63] *etc.*.

These attempts are less advanced than seesaw - GUT scenario. They provide a context with interesting possibilities for construction of specific models.

7. New symmetry of Nature?

There are various approaches to perform analysis of the mixing and mass matrices. One can search for particular features of the matrices like equalities, zeros and hierarchies of its elements. Those may testify for certain exact or approximate symmetries. One can try to decompose matrices into the dominant structure and small corrections, identify small parameters, *etc.*

What are results of this "bottom-up" analysis?

The data show that two types of mixing matrices or the corresponding mass matrices can play the role of the dominant structures.

7.1. Bi-maximal mixing [64]

$$U_{bm} \equiv U_{23}^m U_{12}^m = \frac{1}{2} \begin{pmatrix} \sqrt{2} & \sqrt{2} & 0 \\ -1 & 1 & \sqrt{2} \\ 1 & -1 & \sqrt{2} \end{pmatrix}. \tag{89}$$

Identification $U_{PMNS} = U_{bm}$ is not possible due to strong (5 - 6) σ deviation of the 1-2 mixing from maximal. However, U_{bm} can play a role of matrix in the lowest order. Correction can originate from the charged lepton sector (mass matrix), so that $U_{PMNS} = U' U_{bm}$ and in analogy with quark mixing $U' \approx U_{12}(\theta_C)$. It generates simultaneously deviation of the 1-2 mixing from maximal and non-zero 1-3 mixing, which are related.

7.2. Tri-bimaximal mixing [65]

$$U_{tbm} \equiv U_{23}^{m} U_{12}(\theta_{12}) = \frac{1}{\sqrt{6}} \begin{pmatrix} 2 & \sqrt{2} & 0 \\ -1 & \sqrt{2} & \sqrt{3} \\ 1 & -\sqrt{2} & \sqrt{3} \end{pmatrix}, \tag{90}$$

where $\sin^2\theta_{12} = 1/3$. Here ν_2 is tri-maximally mixed: in the middle column three flavors mix maximally, whereas ν_3 (third column) is bi-maximally mixed. This matrix is in a good agreement with data, in particular, $\sin^2\theta_{12}$ is close to the present best fit value 0.31.

7.3. Neutrino mass and horizontal symmetry

Do the results on neutrino masses and mixing indicate certain regularities or symmetry? Can the dominant structures of the mass matrix be explained by a symmetry with the sub-dominant elements appearing as a result of violations of the symmetry? Is the neutrino mass matrix consistent with symmetries suggested for quarks? In this context the following symmetries have been considered.

1). $L_e - L_\mu - L_\tau$ [67]. This symmetry supports, in particular, the structure with an inverted mass hierarchy. However, the rather large element m_{ee} required by the data shows strong violation of this symmetry.

2). Discrete symmetries: A_4 [68], S_3 [70], Z_4 [71], and D_4 [72] see also [73]. They reproduce successfully the dominant structures of the mass matrix the.

Both classes of symmetries 1) and 2) typically treat quarks and leptons differently.

3). $U(1)$ [74]: In the Froggatt-Nielsen context [75] this symmetry can describe mass matrices of both quarks and leptons. The symmetry can explain general structure of the mass matrix - hierarchy of its elements. However, the predictability of this approach is substantially restricted by unknown coefficients (prefactors) of the order 1 (1/2 - 2) in front of powers of the expansion parameter (usually - Cabibbo angle). The outcome is that the mixing pattern depends substantially on values of these unknown prefactors. Furthermore, the $U(1)$ charges should be considered as discrete free parameters.

4). $SU(2)$,[76] $SO(3)$,[77], and $SU(3)$[78] require a complicated Higgs sector to break the symmetry. Often models are too restrictive and predictions are on the borders of allowed regions. The problem of Yukawa coupling structure here is reduced to the problem of complicated scalar potential which should produce certain alignment of VEV's.

7.4. Symmetry case.

What testifies for the symmetry in the neutrino sector?

(1) Maximal 2-3 mixing

(2) Zero (small) 1-3 mixing;

(3) Particular value 1-2 mixing.

Clearly strong degeneracy of the mass spectrum, if established, will imply symmetry.

It was observed some time ago that the two facts: maximal 2-3 mixing and zero 1-3 mixing can originate both from the same symmetry: invariance of the neutrino mass matrix under $\nu_\mu - \nu_\tau$ permutations in the flavor basis [66]. This permutation symmetry can be a part of larger symmetry which includes also ν_e.

In this connection the flavor symmetry A_4 looks very appealing [68]. It has one triplet representation and three different singlet representations, $\mathbf{1}, \mathbf{1}', \mathbf{1}''$, which provides with enough freedom to explain data. Three leptonic doublets form the triplet of A_4: $L_i = (\nu_i, l_i) \sim \mathbf{3}$, $i = 1, 2, 3$. Required lepton mixing is generated due to different A_4 transformation properties of the right handed components of charged leptons and neutrinos. It is this difference which eventually leads to mixing. In some models: $l_i^c \sim \mathbf{1},\ \mathbf{1}',\ \mathbf{1}''$, whereas $N_i^c \sim \mathbf{3}$. In other models *vice versa*: $l_i^c \sim \mathbf{3}$, $N_i^c \sim \mathbf{1},\ \mathbf{1}',\ \mathbf{1}''$.

Let us consider two examples of the models which illustrate existing achievements and problems.

1). Model A [68, 69]. The right handed components of charged leptons are three different singlets: $l_i^c \sim \mathbf{1},\ \mathbf{1}',\ \mathbf{1}''$. In contrast, the RH components of neutrinos form triplet of A_4: $N_i^c \sim \mathbf{3}$. This is one of the most important differences.

Higgs doublets, are invariant under A_4: $H_{1,2} \sim \mathbf{1}$. (This leads to necessity of introduction of new charged leptons; an alternative would be A_4 triplet of the Higgs bosons.) To construct A_4-invariant Yukawa couplings for charged leptons one needs to introduce Higgs EW singlets which transform as triplets of A_4: $\xi_i \sim \mathbf{3}$. Both neutrinos and charged leptons get masses via the see-saw but the chain of couplings for the two are substantially different. For charge leptons one needs to introduce new heavy charged leptons $E_i, E_i^c \sim \mathbf{3}$ and the chain of couplings is

$$l_i - \langle H_1 \rangle - E_i^c - [M_E] - E_i - \langle \xi_i \rangle - l_i^c. \tag{91}$$

The mixing is generated in the last step by ξ_i. For neutrinos the mass is formed as

$$\nu_i - \langle H_2 \rangle - N_i^c - [M_M] - N_i^c - \langle H_2 \rangle - \nu_i. \tag{92}$$

Extra symmetry is required to forbid unwanted couplings.

The A_4 is broken by VEV of ξ_i which couples to charged leptons and not to neutrinos. This and also the fact that different RH components l_i^c transform according to different singlet representations allows one to reach the goals:

- generate different masses for different charged leptons;
- obtain mixing of charged leptons of specific form which does not depend on mass eigenvalues:

$$U_L = U_{tm} \equiv \begin{pmatrix} 1 & 1 & 1 \\ 1 & \omega & \omega^2 \\ 1 & \omega^2 & \omega \end{pmatrix}, \qquad \omega \equiv e^{-2i\pi/3}. \tag{93}$$

Note, in this way we produce mixing matrix which does not depend on masses.

Neutrino mass matrix is diagonal and degenerate. So, in the flavor basis (where the charged leptons are diagonal), the neutrino mass matrix has the form

$$m_0 \propto U_L^T U_L = \begin{pmatrix} 1 & 0 & 0 \\ 0 & 0 & 1 \\ 0 & 1 & 0 \end{pmatrix}. \tag{94}$$

This matrix gives maximal 2-3 mixing and zero 1-3 mixing. However corrections should be introduced to generate mass split and 1-2 mixing.

It is interesting that in the same context the mixing matrix of quarks is given by $U_L^\dagger U_L = I$ and the CKM matrix should appear due to corrections. That realizes an idea that strong difference of the quark and lepton mixings appears because in zero order of some approximation the quark mixing is zero whereas the lepton mixing is non-zero and large. The large lepton mixing is related to the Majorana nature of neutrinos. To generate neutrino mass split 1-2 leptonic mixing and quark mixing one need to introduce corrections to the above mass matrices. In [69] the radiative mechanism has been proposed to generate these corrections.

Model B: Getting tribimaximal mixing [79]. It is modification of the model A: specifically - modification of the Majorana mass matrix of the RH neutrinos. The charged lepton sector and mechanism of generation of masses coincide with those of the Model A. Additional Higgs multiplets are introduced: A_4 triplet (and SM singlet) ξ'_i and two singlets $S_{1,2}$ which couple to the RH neutrino only.

The scheme of neutrino mass generation is

$$\nu_i - \langle H_2 \rangle - N_i^c - (\langle \xi_2 \rangle, \langle S_{1,2} \rangle) - N_i^c - \langle H_2 \rangle - \nu_i. \tag{95}$$

This produces non-diagonal RH mass matrix which (via seesaw) leads to light neutrino mass matrix with maximal 1-3 rotation: $U_\nu = V_{13}^m$. For this the crucial condition is that only the second component of ξ_2 acquires non-zero VEV.

As a result after rephasing the lepton mixing matrix equals

$$U_{PMNS} = U_{tm} V_{13}^m = U_{tbm}. \tag{96}$$

It is interesting that tri/bimaximal mixing equals the product of the trimaximal and maximal 1-3 rotations.

On symmetry approach. The main question here is whether the "neutrino" symmetries are accidental or real, that is, have some physics behind. Models proposed so far are rather complicated with a number of *ad hoc* assumptions. It is difficult to include quarks in these models. Further (Grand) unification looks rather problematic. Asymmetries between neutrinos and leptons are embedded into theory from the beginning. This shows the price one should to pay for realization of the "neutrino" symmetries.

Furthermore, the facts behind the symmetries - maximal 2-3 mixing and relatively small 1-3 mixing are not yet well established. Still significant deviation of 2-3 mixing is possible and 1-3 mixing can be not so small. Structure of the neutrino mass matrix depends substantially on these deviations. So, it may happen that symmetry constructions are simply misleading.

On the other hand if symmetries are not accidental, they have consequences of the fundamental importance as the models constructed show. New structures and particles are predicted, unification path may differ substantially from what we are considering now, *etc.*. The symmetries may give some clue for understanding fermion masses in general.

The key question is how to test this? Obviously, we need to search for and measure deviations: of 2-3 mixing from maximal, D_{23}, and 1-3 mixing, $\sin\theta_{13}$, from zero. In the context of specific models the deviations (though small) are expected anyway. The facts we are discussing can originate from the same symmetry and violation of this symmetry will lead then to relations between D_{23} and $\sin\theta_{13}$.

8. Leptons and Quarks

There is apparent correspondence between quarks and leptons. Each quark has its own counterpartner in the leptonic sector. Leptons can be treated as the 4th color [80] following the Pati-Salam $SU(4)$ unification symmetry. Unification is possible, so that quarks and leptons form multiplets of the extended gauge group. The most appealing one is SO(10) [81], where all known components of quarks and leptons (including the RH neutrinos) form unique 16-plet. It is difficult to believe that these features are accidental. Though it is not excluded that the quark-lepton connection has some more complicated form, e.g., of the quark - lepton complementarity [82, 83]. We will consider the quark-lepton symmetry and unification later.

8.1. Comparing results

The mixing patterns of leptons and quarks is strongly different: the lepton mixings are large whereas quark mixings are small. The only common feature is that the 1-3 mixing (between the

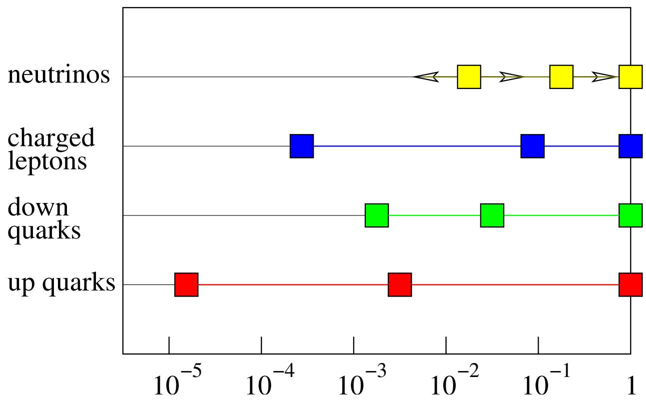

Figure 12. Mass hierarchies of quarks and leptons. The mass of heaviest fermion of a given type is taken to be 1.

"remote" generations) is small in both cases. Two other angles look complementary in a sense that they sum up to maximal mixing:

$$\theta_{12} + \theta_C \approx \frac{\pi}{4}, \tag{97}$$

and similar approximate relation is satisfied for the 2-3 mixings. For various reasons it is difficult to expect precise relation but qualitatively one can say that, the 2-3 mixing in the lepton sector is close to maximal because the corresponding quark mixing is very small, the 1-2 mixing deviates from maximal substantially because the 1-2 (Cabibbo) quark mixing is relatively large. It seems that for the third angle we do not expect simple relation and apparently the quark feature $\theta_{13} \sim \theta_{12} \times \theta_{23}$ does not work in the lepton sector.

The ratio of neutrino masses (67) can be compared with ratios for charged leptons and quarks (at m_Z scale): $m_\mu/m_\tau = 0.06$, $m_s/m_b = 0.02 - 0.03$, $m_c/m_t = 0.005$. The neutrino hierarchy - see eq. (67) (if exists at all - still the degenerate spectrum is not excluded) is the weakest one. This is consistent with possible mass-mixing relation: large mixings are associated to weak mass hierarchy.

In fig. 12 we show the mass ratios for three generations. The strongest hierarchy and geometric relation $m_u \times m_t \sim m_c^2$ exist for the upper quarks. Apart from that no simple relations show up.

What is behind this picture? Symmetry, regularities, relation? In the quark sector we can speak about fermion families with weak interfamily connection (mixing) which means strong flavor alignment. In the lepton sector the alignment is weaker.

Furthermore, peculiar situation with fermion masses is that spectra have small number of states (levels) - 3 (in contract to atomic or nuclear levels), and on the other hand there is no simple relations between parameters of spectra. This may indicate that physics behind fermion masses is rather complicated. It looks like the observed pattern is an interplay of some regularities and randomness ("anarchy").

8.2. Quark-lepton universality

The picture described in the previous section is still consistent with the approximate quark-lepton symmetry or universality. However, the symmetry is realized in terms of mass matrices (matrices of the Yukawa couplings) and not in terms of observables - mass ratios and mixing angles.

The key point is that similar mass matrices can lead to substantially different mixing angles and masses (eigenvalues) if the matrices are nearly singular (rank-1) [84, 85]. The singular matrices are "unstable" in a sense that small perturbations can lead to strong variations of mass ratios and mixing angles (the latter - in the context of seesaw.

Let us consider the universal structure for the Yukawa coupling matrices of all quarks and leptons [85]:

$$Y_u \sim Y_d \sim Y_D \sim Y_M \sim Y_L \sim Y_0, \tag{98}$$

where Y_D is the Dirac type neutrino Yukawa matrix, Y_M is the Majorana type matrix for the RH neutrinos and Y_0 is the singular matrix. As an important (though may be not the best) example we can take

$$Y_0 = \begin{pmatrix} \lambda^4 & \lambda^3 & \lambda^2 \\ \lambda^3 & \lambda^2 & \lambda \\ \lambda^2 & \lambda & 1 \end{pmatrix}, \qquad \lambda \sim 0.2 - 0.3. \tag{99}$$

This matrix has only one non-zero eigenvalue and since all matrices have the same structure, the mixing is zero.

Let us introduce perturbations ϵ in the following form

$$Y_{ij}^f = Y_{ij}^0(1 + \epsilon_{ij}^f), \quad f = u, d, e, \nu, N, \tag{100}$$

where Y_{ij}^0 is the element of the original singular matrix. This form can be justified, *e.g.* in the context of the Froggatt-Nielsen mechanism [75]. (The key element is the form of perturbations (100) which distinguishes the ansatz (99) from other possible schemes with singular matrices.) It has been shown that small perturbations $\epsilon \leq 0.25$ are enough to explain large difference in mass hierarchies and mixings of quarks and leptons [85].

Smallness of neutrino mass is explained by the seesaw mechanism. Furthermore, nearly singular matrix of the RH neutrinos leads to enhancement of the lepton mixing [58] and to flip of sign of mixing angle which comes from diagonalization of the neutrino mass matrix. So, the angles from the charged leptons and neutrinos sum up, whereas in quark sector mixing angles from up and down quark mass matrices subtract.

Keeping this possibility in mind one can consider the following "working" hypothesis:
1). No particular "neutrino" symmetry exists, and in general one expects some deviation of the 2-3 mixing from maximal as well as non-zero 1-3 mixing. Nearly maximal 2 -3 mixing would be accidental in this case.
2). Seesaw mechanism with the scale of RH neutrino masses $M \sim (10^7 - 10^{15})$ GeV explains smallness of neutrino mass. The upper part of this range is close to the GU scale and can be considered as indication of the Grand Unification.
3). The quark-lepton unification or Grand Unification are realized in some form, e.g. $SO(10)$.
4). The quark-lepton symmetry is (weakly) broken and some observable consequences like, $m_b = m_\tau$, exist.
5). Large lepton mixing is a consequence of the seesaw type-I mechanism - the seesaw enhancement of lepton mixing due to special structure of the RH neutrino mass matrix, (or/and of the contribution from the type II seesaw).
6). Flavor (family) symmetry or/and physics of extra dimensions determine this special structure.

Testing scenario. This is the key question which requires essentially the test of existence of the heavy Majorana RH neutrinos. The RH neutrinos can produce renormalization effects above the scale of their masses: between M_R and, say, the GUT scale. In particular, they can renormalize the $m_b - m_\tau$ mass relation[86] which leads to the observable effect in the assumption of $m_b - m_\tau$ unification at the GUT scale. Another possibility is that the renormalization due to RH neutrinos modifies masses and mixing of the light neutrinos, e.g., enhances the mixing [87].

Several indirect) possibilities to test seesaw are known at present:

- Leptogenesis [88];
- Neutrinoless beta decay;
- Rare lepton number violating decays [89].

Radical solution - the "Low scale seesaw" with masses of the RH neutrinos at 1 TeV or 1 keV or even 1 eV have been proposed. One of the motivations is to make things testable.

8.3. Quark-lepton complementarity (QLC)

The complementarity condition (97) would require certain modification of the picture described above [82, 83]. The latest determination of the solar mixing angle gives

$$\theta_{12} + \theta_C = 46.7^\circ \pm 2.4^\circ \quad (1\sigma)$$

which is consistent with maximal mixing angle within 1σ. If not accidental, the QLC relation implies that there is some structure in the theory which generates maximal or bi-maximal mixing and it should be non-trivial quark-lepton connection which communicates the quark mixing to the lepton sector. The fact that for the 2-3 mixings the approximate complementarity is also fulfilled hints some more serious reason than just numerical coincidence.

A general scheme is that

$$\text{“lepton mixing} = \text{bi} - \text{maximal mixing} - \text{CKM}''. \tag{101}$$

There is a number of non-trivial conditions for the exact QLC relation to be realized.

(i) Order of rotations: apparently U_{12}^m and $U_{12}^{CKM\dagger}$ should be attached

$$U_{PMNS} \equiv U_L^\dagger U_\nu = ...U_{23}^m ... U_{12}^m U_{12}^{CKM\dagger} \tag{102}$$

(two last rotations can be permuted). Different order leads to corrections to the exact QLC relation;

(ii) Matrix with CP violating phases should not appear between $U_{12}^{CKM\dagger}$ and U_{12}^m, or the corresponding mixing should be small enough.

(iii) Presumably the quark-lepton symmetry which leads to the QLC relation is realized at high mass scales. Therefore the renormalization group effects should be small enough, *etc.*.

Let us describe two possible scenarios which differ by origin of the bi-maximal mixing and lead to different predictions [83].

1). QLC1: In the symmetry basis, the bi-maximal mixing is generated by the neutrino mass matrix, presumably due to seesaw. The charged lepton mass matrix produces the CKM mixing as a consequence of the q-l symmetry: $m_l \approx m_d$. In this case the order of matrices (102) is not realized (U_{12}^{CKM} should be permuted with U_{23}^m), and consequently the QLC relation is modified:

$$\sin\theta_{12} = \sin(\pi/4 - \theta_C) + 0.5 \sin\theta_C(\sqrt{2} - 1). \tag{103}$$

Numerically we find $\tan^2\theta_{12} = 0.495$ which is practically indistinguishable from the tri-bimaximal mixing with $\tan^2\theta_{12} = 0.50$.

2). QLC2: Maximal mixing comes from the charged lepton mass matrix and the CKM mixing originates from the neutrino mass matrix due to the q-l symmetry: $m_D \sim m_u$ (assuming also that in the context of seesaw the RH neutrino mass matrix does not influence mixing). In this case the QLC relation is satisfied precisely: $\sin\theta_{12} = \sin(\pi/4 - \theta_C)$, and the 1-3 mixing is very small.

There are two main issues related to the QLC relation:
(1) origin of the bi-maximal mixing;
(2) mechanism of propagation of the CKM mixing from the quark to the lepton sector. The problem here is large difference of mass ratios in the quark and lepton sectors: $m_e/m_\mu = 0.0047$, $m_d/m_s = 0.04 - 0.06$, as well as difference of masses of muon and s-quark at the GU scale. This means that mixing should weakly depend or be independent on masses.

The mass matrices are different for quarks and leptons and "propagation" of the CKM mixing leads to corrections to the QLC relation of the order $\Delta\theta_{12} \sim \theta_C m_d/m_s \sim 0.5 - 1.0^\circ$ [83].

The Cabibbo mixing can be transmitted to the lepton sector in more complicated way (than via the q-l symmetry). In fact, $\sin\theta_C$ may turn out to be the generic parameter of theory of fermion masses and therefore to appear in various places: mass ratios, mixing angles. The relation: $\sin\theta_C \approx \sqrt{m_\mu/m_\tau}$ is in favor of this possibility. On the other hand, this relation may indicate that the QLC relation is accidental. Indeed, it can be rewritten as a pure leptonic relation $\theta_{12} + \theta_{\mu\tau} = \pi/4$, where $\tan\theta_{\mu\tau} \equiv \sqrt{m_\mu/m_\tau}$. Though this relation may even be more difficult to realize.

So, if not accidental the QLC relation may have two different implications: One includes the quark-lepton symmetry, existence of some additional structure which produces the bi-maximal mixing, and mass matrices with weak correlation of the mixing angles on mass eigenvalues. Alternatively, it may imply certain flavor physics with $\sin\theta_C$ being the "quantum" of this physics.

9. See-saw and GUT's

9.1. Seesaw: variations on the theme

The number of RH neutrinos (or SM singlets involved in generation of neutrino mass) can differ from 3. In fact minimal number of the RH neutrinos needed to generate masses of light neutrinos via type I seesaw is 2. In this case we have the 3×2 see-saw [90]. Such a possibility can be realized in the limit when one of the RH neutrinos is very heavy: $M \sim M_{Pl}$, being, unprotected by, *e.g.*, the $SU(2)_H$ horizontal symmetry. It leads to one massless LH neutrino and smaller number of free parameters.

The number of SM singlets involved in the neutrino mass generation can be larger than 3, moreover additional singlets may not be related to the family structure.

Alternatively, three additional singlets, S, which belong to families, can couple to the RH neutrinos. In the latter case the double see-saw can be realized [91].

In the basis (ν, ν^c, S) the mass matrix may have the form

$$\begin{pmatrix} 0 & m_D & 0 \\ m_D^T & 0 & M \\ 0 & M^T & M_S \end{pmatrix} \tag{104}$$

due to certain symmetries including the lepton number one. It leads to the light neutrino masses:

$$m = -m_D^T (M^{-1})^T M_S M^{-1} m_D. \tag{105}$$

Two interesting limits are:

(i) $M_S \ll M$, it allows one to reduce all high mass scales for the same values of the light neutrino masses. In this case in each generation one has heavy pseudoDirac neutrino with mass $\sim M$. Such a possibility has some justification in the string theory.

(ii) $M_S \gg M$ produces the "cascade" seesaw: the mass of RH neutrino also appears as a result of seasaw:

$$M_R = M M_S^{-1} M^T. \tag{106}$$

For $M_S = M_{Pl}$, and $M = M_{GU}$ we obtain the required intermediate mass scale for these masses $M_R = M_{GU}^2/M_{Pl} = (10^{12} - 10^{14})$ GeV.

Seesaw type III [92]. Three additional singlets can couple both to the LH and RH neutrinos, so that the mass matrix in the basis (ν, N, S) becomes

$$m_\nu \approx \begin{pmatrix} 0 & m_D & m \\ m_D^T & 0 & M \\ m^T & M^T & 0 \end{pmatrix}, \tag{107}$$

where $m \sim v_{EW}$. The lepton number is violated in this system since S couples with both ν and N which have the lepton numbers +1 and -1 correspondingly.

The Majorana mass matrix of light neutrinos becomes

$$m_\nu = m_D (M^T)^{-1} m^T + (transponent). \tag{108}$$

The new feature of this matrix is that it is linearly proportional to the Dirac mass matrix in contrast to the seesaw type I. Here the cancellation of the mass hierarchies occurs if $M \propto m$. The spectrum of the heavy components consists of three pairs of the preudoDirac neutrinos which can lead to the resonance leptogenesis.

Screening of Dirac structure. The quark -lepton symmetry manifests as certain relation (similarity) between the Dirac mass matrices of quarks and leptons, and it is this feature which creates problem for explanation of strongly different mixings and possible existence of the "neutrino" symmetries. Let us consider an extreme case when in spite of the q-l unification, the Dirac structure in the lepton sector is completely eliminated - "screened" [93].

Consider the double seesaw structure (104). Suppose that due to some horizontal symmetry or Grand unification which includes also new singlets S, the two Dirac mass matrices in the double seesaw are proportional each other:

$$M_D = A^{-1} m_D, \qquad A \equiv v_{EW}/V_{GU}. \tag{109}$$

Then they cancel each other in (**??**) and for the light neutrinos we obtain

$$m_\nu = A^2 M_S. \tag{110}$$

That is, the structure of light neutrino mass matrix is determined by M_S immediately and does not depend on the Dirac mass matrix. In this case the seesaw mechanism provides with the scale of neutrino masses but not the flavor structure of the mass matrix. It can be shown that at least in SUSY version the radiative corrections do not destroy screening [93].

Structure of the light neutrino mass matrix depends now on M_S which can be related to some physics at the Planck scale, and consequently lead to "unusual" neutrino properties. In particular, (i) M_S can be the origin of the "neutrino" symmetry; (ii) the matrix $M_S \propto I$ leads to the quasi-degenerate spectrum; (iii) M_S can be the origin of the bi-maximal or maximal mixing thus leading to the QLC relation if the charged lepton mass matrix generates the CKM rotation.

9.2. GUT's and neutrino mass

GUT's naturally provides us with

- the RH neutrino components,
- large mass scale,
- lepton number violation.

So, it contains all ingredients needed for realization of the seesaw mechanism. What else GUT's can do for neutrinos? Generically GUTs give relations between masses and mixings of the quarks and leptons (see for review [94]). Nature of the relations, however, is model dependent. It is determined by the gauge symmetry, representations of fermions and Higgses and number of various Higgs representations.

The highest predictivity is of course when all fermions are in the same multiplet (like **16**-plet of SO(10)) and only one higgs multiplet generates masses (unless some additional principles are introduced on the top of GUT). At this point we can discuss "Minimal $SO(10)$" model with only two Higgs multiplets which generate the fermion masses: $\mathbf{10}_H$ and $\mathbf{1\bar{2}6}_H$ [95]. With only one $\mathbf{10}_H$ the predictions are the most stringent but contradict observations: all up masses are equal, all down masses are equal, mass hierarchies are the same for all fermions and there is no mixing.

So one needs to introduce other sources of fermion masses and the straightforward step is to add $\mathbf{1\bar{2}6}_H$. Now predictivity becomes weaker: instead of equalities of masses we get the "sum rules" [96].

Indeed, with $\mathbf{10}_H$ and $\mathbf{1\bar{2}6}_H$ the following mass matrices are generated:

$$\begin{aligned} M_u &= Y_{10} v_{10}^u + Y_{126} v_{126}^u \\ M_d &= Y_{10} v_{10}^d + Y_{126} v_{126}^d \\ M_l &= Y_{10} v_{10}^d - 3Y_{126} v_{126}^d \\ M_\nu &= Y_{126} k, \end{aligned} \tag{111}$$

where Y_{10} and Y_{126} are the matrices of the Yukawa couplings and v_{10}^u, v_{10}^d and v_{126}^u, v_{126}^d VEV's are the VEV's of $\mathbf{10}_H$ and $\mathbf{1\bar{2}6}_H$ correspondingly. It is assumed in (111) that seesaw type II, (due to the EW triplet in $\mathbf{1\bar{2}6}_H$) gives the main contribution to neutrino mass and k denotes the induced VEV of this triplet.

Excluding product of Yukawas and VEV's in the above system of equations we find the sum rule

$$M_\nu \propto M_l - M_d \tag{112}$$

- relation between mass matrices of the charged leptons, down quarks and neutrinos. The $b-\tau$ unification (that is $m_b \approx m_\tau$ at the GUT scale) implies $(M_l)_{33} \approx (M_d)_{33}$. Consequently from the relation (112) we obtain $(M_\nu)_{33} \approx 0$. In fact, numerically $(M_\nu)_{33} \approx (M_\nu)_{22}$. This leads to large 2-3 leptonic mixing. Notice that with Higgs sector containing both 10 plet and 126 plet, the $b-\tau$ unification is not the consequence of theory but phenomenological input.

Considering the sum rule (112) for the matrices of second and third generations one finds [97]

$$\tan 2\theta_{23} = \frac{2\sin\theta_{23}^q}{2\sin^2\theta_{23}^q - (m_b - m_\tau)/m_b}. \tag{113}$$

Here θ_{23}^q is the quark mixing m_b is the mass of b-quark and m_τ is the mass of τ-lepton. This relation connect large leptonic 2-3 mixing and an approximate equality, $m_b \approx m_\tau$, at the GUT scale. Indeed, only for $(m_b - m_\tau)/m_b \ll 1$ one gets large θ_{23}. Essentially, the point is that $\mathbf{1\bar{2}6}_H$ should give small contribution to the 33 element of the mass matrix, otherwise masses m_b and m_τ will be different. In fact, numerically one needs to have $(Y_{126})_{33} \sim (Y_{126})_{22}$. In the assumption that $\mathbf{1\bar{2}6}_H$ gives the main contribution to the neutrino mass this implies large neutrino 2-3 mixing.

It seems the minimal SO(10) has problems in explaining all the fermion masses so that further extension is needed. Introduction of 120_H in addition leads to further loss of predictivity.

10. Conclusion

Last 5 - 7 years was epoch of great achievements in neutrino physics:

- discovery of neutrino oscillations,
- resolution of the solar neutrino problem and establishing the matter effect,
- measurements of neutrino parameters.

As a result of these discoveries amazing pattern of the lepton mixing has emerged.

Clear program of future phenomenological and experimental studies has been elaborated. At the same time implications and identification of the underlying physics is a big challenge, and it may happen that something important (in principles and context) is still missed. Substantial input from high energy experiments astrophysics and cosmology will be helpfull.

The hope is that neutrinos will uncover something simple and illuminating before we will be lost in the string landscape.

11. References

[1] R. E. Marshak and R. N. Mohapatra, *Phys. Lett.* B **91** (1980) 222.
[2] B. Pontecorvo, Zh. Eksp. Theor. Fiz. **33** (1957); *ibidem* **34** (1958) 247.
[3] Z. Maki, M. Nakagawa and S. Sakata, Prog. Theor. Phys. **28** (1962) 870.
[4] B. Pontecorvo, ZETF, **53**, 1771 (1967) [Sov. Phys. JETP, **26**, 984 (1968)]; V. N. Gribov and B. Pontecorvo, Phys. Lett. **28B** (1969) 493.
[5] L. Wolfenstein, Phys. Rev. D**17** (1978) 2369; in *"Neutrino -78"*, Purdue Univ. C3, (1978), Phys. Rev. **D20** (1979) 2634.
[6] S. P. Mikheyev and A. Yu. Smirnov, Sov. J. Nucl. Phys. **42** (1985) 913; Nuovo Cim. **C9** (1986) 17; S.P. Mikheev and A.Yu. Smirnov, Sov. Phys. JETP **64** (1986) 4.
[7] N. Cabibbo, Summary talk given at 10th Int. Workshop on Weak Interactions and Neutrinos, Savonlinna, Finland, June 1985.
[8] H. Bethe, Phys. Rev. Lett. **56** (1986) 1305.
[9] A. Messiah, Proc. of the 6th Moriond Workshop on Massive Neutrinos in Particle Physics and Astrophysics, eds O. Fackler and J. Tran Thanh Van, Tignes, France, Jan. 1986, p. 373; S. P. Mikheev and A. Y. Smirnov, Sov. Phys. JETP **65**, 230 (1987).
[10] S. J. Parke, Phys. Rev. Lett. **57** (1986) 1275.
[11] W. C. Haxton, Phys. Rev. Lett. **57** (1986) 1271.
[12] P. C. de Holanda, Wei Liao, A. Yu. Smirnov, Nucl. Phys. B**702** (2004) 307.
[13] B. T. Cleveland *et al.*, Astrophys. J. **496** (1998) 505.
[14] J. Hosaka *et al.* [Super-Kamkiokande Collaboration], arXiv:hep-ex/0508053.
[15] J. N. Abdurashitov *et al.* [SAGE Collaboration], J. Exp. Theor. Phys. **95** (2002) 181 [Zh. Eksp. Teor. Fiz. **122** (2002) 211].
[16] W. Hampel *et al.* [GALLEX Collaboration], Phys. Lett. B **447** (1999) 127.
[17] M. Altmann *et al.* [GNO COLLABORATION Collaboration], Phys. Lett. B **616** (2005) 174
[18] SNO Collaboration (B. Aharmim et al.). *Phys. Rev.* C **72** (2005) 055502.
[19] J. N. Bahcall, M.H. Pinsonneault, Phys. Rev. Lett. **92** (2004) 121301; J. N. Bahcall, A. M. Serenelli and S. Basu, astro-ph/0511337.
[20] P. C. de Holanda, A.Yu. Smirnov, Astropart. Phys. **21** (2004) 287.
[21] A. N. Ioannisian and A.Yu. Smirnov, Phys. Rev. Lett. **93** (2004) 241801.
[22] T. Araki *et al.* [KamLAND Collaboration], Phys. Rev. Lett. **94** (2005) 081801.
[23] Super-Kamiokande Collaboration (Y. Ashie et al.), *Phys. Rev.* D **71** (2005) 112005.
[24] M. Ambrosio *et al.* [MACRO Collaboration], Eur. Phys. J. C **36** (2004) 323.
[25] M. C. Sanchez *et al.* [Soudan 2 Collaboration], Phys. Rev. D **68** (2003) 113004.
[26] [MINOS Collaboration], arXiv:hep-ex/0512036.
[27] Y. Ashie *et al.* [Super-Kamiokande Collaboration], Phys. Rev. Lett. **93** (2004) 101801

[28] M. C. Gonzalez-Garcia, M. Maltoni, A. Yu. Smirnov, *Phys. Rev.* D **70** (2004) 093005.
[29] G. L. Fogli et al, hep-ph/0506083.
[30] E. Aliu *et al.* [K2K Collaboration], Phys. Rev. Lett. **94** (2005) 081802.
[31] M. Apollonio *et al.*, Eur. Phys. J. C **27** (2003) 331.
[32] A. Strumia, F. Vissani, *Nucl. Phys.* B **726** (2005) 294.
[33] V. M. Lobashev *et al.*, Nucl. Phys. Proc. Suppl. **91** (2001) 280.
[34] C. Kraus *et al.*, Eur. Phys. J. C **40** (2005) 447.
[35] A. Osipowicz *et al.* [KATRIN Collaboration], arXiv:hep-ex/0109033.
[36] H.V. Klapdor-Kleingrothaus *et al.*, *Eur. Phys. J.* A **12**, 147 (2001); A. M. Bakalyarov *et al.,* talk given at *the 4th International Conference on Non-accelerator New Physics* (NANP 03), Dubna, Russia, 23-28 Jun. 2003, hep-ex/0309016.
[37] H.V. Klapdor-Kleingrothaus *et al., Mod. Phys. Lett.* A **16** (2001) 2409.
[38] H.V. Klapdor-Kleingrothaus, et al, *Phys. Lett.* B **586** (2004) 198.
[39] U. Seljak et al.. *Phys. Rev.* D **71** (2005) 103515.
[40] A. Aguilar *et al.*, (LSND Collaboration) *Phys. Rev.* D **64** (2001) 112007.
[41] B. Armbruster, *et al.*, (KARMEN), *Phys. Rev. Lett.*, **90**, 181804 (2003).
[42] K. S. Babu and S. Pakwasa, hep-ph/0204226.
[43] G. Barenboim, L. Borissov, J. Lykken, hep-ph/0212116.
[44] A. Strumia, *Phys. Lett.* B **539**, 91 (2002).
[45] M.C. Gonzalez-Garcia, M. Maltoni T. Schwetz, *Phys. Rev.* D **68**, 053007 (2003).
[46] O. L. G. Peres, A.Yu. Smirnov, *Nucl. Phys.* B **599** (2001) 3.
[47] M. Sorel, J. Conrad, M. Shaevitz, Phys. Rev. D **70** (2004) 073004.
[48] V. Barger, D. Marfatia, K. Whisnant, Phys. Lett. B **576** (2003) 303.
[49] D. B. Kaplan, A. E. Nelson and N. Weiner, Phys. Rev. Lett. **93** (2004) 091801.
[50] S. Palomares-Ruiz, S. Pascoli and T. Schwetz, JHEP **0509** (2005) 048.
[51] M. H. Shaevitz [MiniBooNE Collaboration], Nucl. Phys. Proc. Suppl. **137** (2004) 46 [arXiv:hep-ex/0407027].
[52] S. Weinberg, Phys. Rev. Lett. **43**, 1566 (1979).
[53] R. Barbieri, J. Ellis and M. K. Gaillard, *Phys. Lett.* B **90** (1980) 249; E. Kh. Akhmedov, Z. G. Berezhiani, G. Senjanović, *Phys. Rev. Lett.* **69** (1992) 3013.
[54] F. Vissani, M. Narayan, V. Berezinsky, *Phys. Lett.* B **571** (2003) 209.
[55] P. Minkowski, Phys. Lett. B **67** (1977) 421, for earlier work see H. Fritzsch, M. Gell-Mann and P. Minkowski, Phys. Lett. B **59** (1975) 256, H. Fritzsch and P. Minkowski, Phys. Lett. B **62** (1976) 72.
[56] M. Gell-Mann, P. Ramond and R. Slansky, in *Supergravity*, eds P. van Niewenhuizen and D. Z. Freedman (North Holland, Amsterdam 1980); P. Ramond, *Sanibel talk*, retroprinted as hep-ph/9809459; T. Yanagida, in *Proc. of Workshop on Unified Theory and Baryon number in the Universe*, eds. O. Sawada and A. Sugamoto, KEK, Tsukuba, (1979); S. L. Glashow, in *Quarks and Leptons*, Cargèse lectures, eds M. Lévy, (Plenum, 1980, New York) p. 707; R. N. Mohapatra and G. Senjanović, *Phys. Rev. Lett.* **44**, (1980) 912.
[57] R. N. Mohapatra and G. Senjanović, *Phys. Rev.* D **23** (1981) 165, C. Wetterich, *Nucl. Phys.* B **187** (1981) 343.
[58] A. Yu. Smirnov, Phys. Rev. D **48** (1993) 3264. M. Tanimoto, Phys. Lett. B **345** (1995) 477; T.K. Kuo, Guo-Hong Wu, Sadek W. Mansour, Phys. Rev. D **61**, 111301 (2000); G. Altarelli F. Feruglio and I. Masina, Phys. Lett. B **472**, 382 (2000); S. Lavignac, I. Masina, C. A. Savoy, Nucl. Phys. B **633**, 139 (2002). A. Datta, F. S. Ling and P. Ramond, Nucl. Phys. B **671** (2003) 383; M. Bando, *et al.,* Phys. Lett. B **580** (2004) 229.
[59] N. Arkani-Hamed, S. Dimopoulos, G. R. Dvali and J. March-Russell, *Phys. Rev.* D **65**, 02432 (2002); K. R. Dienes, E. Dudas and T. Ghergetta, *Nucl. Phys.* B **557** (1999) 25.
[60] Y. Grossman and M. Neubert, *Phys. Lett.* B **474**, (2000) 361.
[61] T. Gherghetta, Phys. Rev. Lett. **92** (2004) 161601.
[62] N. Arkani-Hamed, M. Schmaltz, Phys. Rev. D**61** (2000) 033005.
[63] P.Q. Hung, Phys. Rev. D **67** (2003) 095011.
[64] F. Vissani, hep-ph/9708483; V. D. Barger, et al, Phys. Lett. B **437**, 107 (1998).
[65] L. Wolfenstein, Phys. Rev. D **18**, 958 (1978); P. F. Harrison, D. H. Perkins and W. G. Scott, *Phys. Lett.* B **458**, 79 (1999), *Phys. Lett.* B **530**, 167 (2002).
[66] T. Fukuyama and H. Nishiura, hep-ph/9702253; R. N. Mohapatra and S. Nussinov, *Phys. Rev.* D **60**, 013002 (1999); E. Ma and M. Raidal, *Phys. Rev. Lett.* **87**, 011802 (2001); C. S. Lam, *Phys. Lett.* B **507**, 214 (2001).
[67] S. T. Petcov, *Phys. Lett.* B **110** (1982) 245; R. Barbieri *et al.*, *JHEP* **9812** (1998) 017.
[68] E. Ma, *Mod. Phys. Lett.* A **17**, 2361 (2002); E. Ma, G. Rajasekaran, *Phys. Rev.* D *64* (2001) 113012.
[69] K.S. Babu, E. Ma, J.W.F. Valle, *Phys. Lett.* B **552** (2003) 207.

[70] J. Kubo *et al.*, *Prog. Theor. Phys.* **109** (2003) 795.
[71] E. Ma, G. Rajasekaran, hep-ph/0306264.
[72] W. Grimus, L. Lavoura, hep-ph/0305046.
[73] For some recent publications see: W. Grimus and L. Lavoura, *JHEP* **0508**, 013 (2005); E. Ma, *Mod. Phys. Lett.* A **20**, 2601 (2005).
[74] J. Bijnens C. Wetterich, *Nucl. Phys.* B **292** (1987) 443; M. Leurer, Y. Nir and N. Seiberg, *Nucl. Phys.* B **398** (1993) 319; *ibidem*, **420**, 468 (1994); L. E. Ibanez and G.G. Ross, *Phys. Lett.* B **332**, 100 (1994); P. Binetruy and P. Ramond, *Phys. Lett.* B **350**(1995) 49; for references and recent discussion see G. Altarelli and F. Feruglio, hep-ph/0306265; P. H. Chankowski, K. Kowalska, S. Lavignac and S. Pokorski, Phys. Rev. D **71** (2005) 055004.
[75] C. D. Froggatt and H. B. Nielsen, *Nucl. Phys.* B **147**, 277 (1979).
[76] R. Kuchimanchi and R. N. Mohapatra, *Phys. Rev.* D **66**, 051301 (2002).
[77] R. Barbieri, L. J. Hall, G. L. Kane and G. G. Ross, hep-ph/9901228.
[78] G. Kribs, hep-ph/0304256; S. F. King, *Phys. Lett.* B **520**, 243 (2001); S.F. King, G.G. Ross, *Phys. Lett.* B **574**, 239 (2003).
[79] K. S. Babu and X. G. He, hep-ph/0507217.
[80] J. C. Pati and A. Salam, *Phys. Rev.* D **10**, 275 (1974).
[81] H. Georgi, *In Coral Gables 1979 Proceeding, Theory and experiment in high energy physics*, New York 1975, 329 and H. Fritzsch and P. Minkowski, Annals Phys. **93** 193 (1975).
[82] A. Yu. Smirnov, hep-ph/0402264; M. Raidal, *Phys. Rev. Lett.* **93** (2004) 161801.
[83] H. Minakata, A. Yu. Smirnov, *Phys. Rev.* D **70** (2004) 073009.
[84] E. K. Akhmedov, et al., *Phys. Lett.* B **498**, 237 (2001); R. Dermisek, *Phys. Rev.* D **70**, 033007 (2004).
[85] I. Dorsner, A.Yu. Smirnov, *Nucl. Phys.* B **698** (2004) 386.
[86] F. Vissani, A. Yu. Smirnov, *Phys. Lett.* B **341**, 173 (1994). A. Brignole, H. Murayama, R. Rattazzi, *Phys. Lett.* B **335**, 345 (1994).
[87] M. Lindner, S. Antusch, J. Kersten, M. Lindner, M. Ratz, *Phys. Lett.* B **544**, 1 (2002).
[88] These proceedings.
[89] These proceedings.
[90] P. H. Frampton, S. L. Glashow, T. Yanagida, *Phys. Lett.* B **548**, 119 (2002).
[91] R. N. Mohapatra, *Phys. Rev. Lett.* **56**, 561 (1986); R. N. Mohapatra and J. W. F. Valle, *Phys. Rev.* D **34**, 1642 (1986).
[92] S. M. Barr, Phys. Rev. Lett. **92** (2004) 101601.
[93] M. Lindner, M. A. Schmidt, A. Yu. Smirnov, *JHEP* **0507**, 048 (2005).
[94] For recent review of neutrino masses in GUT see M-C. Chen and K. T. Mahanthappa, Int. J. Mod. Phys. A **18** (2003) 5819.
[95] K. S. Babu and R. N. Mohapatra, Phys. Rev. Lett. **70** (1993) 2845.
[96] B. Bajc, G. Senjanovic and F. Vissani, Phys. Rev. Lett. **90** (2003) 051802.
[97] S. Bertolini, M. Frigerio and M. Malinsky, Phys. Rev. D **70** (2004) 095002.